cemfi

working paper
2603

Unobservable no more: estimating the natural rate of interest under flat IS and Phillips curves

Gabriele Fiorentini
Alessandro Galesi
Rodrigo Peña
Gabriel Pérez Quirós
Enrique Sentana

March 2026

CENTRO DE ESTUDIOS
MONETARIOS Y FINANCIEROS
Casado del Alisal 5, 28014 Madrid, Spain
www.cemfi.es

CEMFI Working Paper No. 2603
March 2026

Unobservable no more: estimating the natural rate of interest under flat IS and Phillips curves

Abstract

We show that the Laubach and Williams (2003) model and its variants in Holston, Laubach and Williams (2017, 2023) cannot estimate the natural rate with finite precision when either the IS curve or the Phillips curve are flat. To solve this unobservability, we propose a simple augmented model with a mean-reverting interest rate gap that considerably narrows the natural rate's confidence bands in those empirically relevant situations. We also assess the ability of the corporate risk premium and the share of working age population to explain movements in the natural rate, but they generate filtered estimates that fluctuate too much.

JEL Codes: E43, E52, C32, C52.

Keywords: Demographics, Kalman filter, observability, risk appetite.

Gabriele Fiorentini
Università di Firenze and RCEA
gabriele.fiorentini@unifi.it

Alessandro Galesi
Idealista
agalesi@idealista.com

Rodrigo Peña
CEMFI
rodrigo.pena@cemfi.edu.es

Gabriel Pérez Quirós
Banco de España
gabriel.perez@bde.es

Enrique Sentana
CEMFI
sentana@cemfi.es

Acknowledgement

This is a substantially revised version of Fiorentini, Galesi, Pérez-Quirós and Sentana (2018). In addition to those acknowledged there, we would like to thank Daniel Buncic, Rodolfo Campos and audiences at the EUI Conference on the Natural Rate of Interest, the XVII Banco de España - CEMFI Workshop and Fulcrum Asset Management for very useful comments and suggestions. The input of the editor, associate editor and a referee have also led to substantial improvements. Of course, the usual caveat applies. Disclaimer: The views expressed herein are those of the authors and not necessarily reflect those of Banco de España or the Eurosystem.

1 Introduction

The natural rate of interest, popularly known as r^*, is loosely understood as the one that neither constrains nor stimulates the economy when it reaches full employment and inflation the prespecified target level. This concept has become very important in the analysis of monetary policy decisions, as highlighted in the recent volume edited by Rush, Orlik and Flanders (2025). At the same time, it is also somewhat elusive and controversial because r^* is not observed, moves over time, and is driven by forces whose precise nature is not well understood.

Although there is no consensus on how to estimate r^*, one of the best known methods relies on the original Laubach and Williams (2003) (LW) macroeconomic model and its refined version in Holston, Lauback and Williams (2017) (HLW17). This "reduced form" model combines data on real GDP, core inflation and the federal funds rate to extract trends in U.S. economic growth and a second latent factor known as z that captures all other unspecified influences on the natural rate of interest.

To inmunise the filtered estimates of r^* against the disruptions created by the COVID-19 pandemic, Holston, Laubach and Williams (2023) (HLW23) refines further the HLW17 model to incorporate:

1. proportional increases in the volatility of the shocks to the output gap and inflation during the last three quarters of 2020 and the whole of 2021 and 2022.

2. a sequence of persistent but temporary supply shocks to potential output during the pandemic as a function of a stringency index of government-imposed restrictions.

Their point estimates are posted every three months on the webpage of the New York Fed https://www.newyorkfed.org/research/policy/rstar from 2005Q1 onwards. They receive substantial attention from the financial media, market participants and top central bankers around the world. Although the associated confidence bands are not publicly available, the New York Fed also posts R code to compute them. In practice, those confidence bands are rather large.

In this regard, we show that the HLW17 and HLW23 models suffer from what is known in the control literature as "unobservability" when either the output gap is insensitive to the difference between the observed interest rate and the natural one (*flat IS curve*), or inflation is insensitive to the output gap (*flat Phillips curve*). Unobservability, a concept introduced in Kalman (1960), means that it would be impossible to recover the initial values of the state variables even if one knew the values of all the model parameters and could see the realisations not only of the observed variables but also of their shocks and measurement errors. Effectively,

this implies that one could not observe the values of the state variables at any particular point in time even in those ideal circumstances.

A trivial example of unobservability would arise in any dynamic model for real GDP if a researcher only used data on nominal GDP but not the price level. The unobservability of the LW and HLW models is far less trivial but nonetheless equally relevant. Intuitively, when the IS curve is flat, the output gap is insensitive to the real interest rate gap, so information about the output gap cannot pinpoint the non-growth component of the natural interest rate, z. In turn, when the Phillips curve is flat, inflation is insensitive to the output gap, which implies that one cannot meaningfully distinguish z from potential output either.

Unfortunately, the problem is not only a theoretical curiosity for those two limiting cases. In practice, the confidence bands around the central estimate of the natural interest rate will be very large in those empirically relevant situations in which either of those curves is close to being flat.

To solve these difficulties, we propose a simple augmented model that restores observability. We do so by merely assuming that the interest rate gap is stationary, which seems very plausible. In this respect, our assumption is consistent with the idea that monetary policy generates temporary deviations from the balanced-growth path of the economy, but it does not alter this path. In practice, our augmented model considerably reduces the width of the confidence bands for the natural rate without changing much its central tendency.

We also investigate whether two economic variables, the corporate risk premium and the fraction of young-age population, which are often cited as observed determinants of the natural interest rate, help explain its movements. Unfortunately, they generate filtered estimates of r^* that fluctuate too much to be plausible even after smoothing our measure of risk appetite. Arguably, this might be due to the fact that the rate of growth in potential output already captures the effects of demographic trends and changes in risk attitudes.

The rest of the paper is organised as follows. In section 2 we present the HLW17 and its COVID-19 immunised version in HLW23, whose observability we analyse in section 3. Then, we present our augmented model in section 4. Finally, we explore potential economic determinants of the non-growth component of the natural rate in section 5. This is followed by our conclusions, and several appendices in which we provide additional details.

2 The HLW model

The first building block of the HLW23 model consists of:

$$\tilde{y}_t = \alpha_{y,1}\tilde{y}_{t-1} + \alpha_{y,2}\tilde{y}_{t-2} - \gamma(\tilde{r}_{t-1} + \tilde{r}_{t-2})/2 + \varepsilon_t^{\tilde{y}}, \quad (1)$$

$$\pi_t = \alpha_\pi \pi_{t-1} + (1-\alpha_\pi)\pi_{t-2,4} + \kappa\tilde{y}_{t-1} + \varepsilon_t^{\pi}. \quad (2)$$

The aggregate demand equation (1) states that the output gap

$$\tilde{y}_t \equiv y_t - y_t^*, \quad (3)$$

namely the deviation of the (log) real GDP, y_t, from its unobserved potential level, y_t^*, depends on both its first two lags and the average over the past two quarters of the realisations of the real interest rate gap,

$$\tilde{r}_t \equiv r_t - r_t^*, \quad (4)$$

defined as the deviation of the observed real interest rate, r_t, from the natural one, r_t^*.

As for the aggregate supply equation (2), it links the observed inflation rate, π_t, to its own lag, the average of its second to fourth lags, $\pi_{t-2,4}$, and the lagged output gap. Finally, $\varepsilon_t^{\tilde{y}}$ and ε_t^{π} are two serially and mutually uncorrelated shocks with variances $\sigma_{\tilde{y}}^2$ and σ_π^2, respectively.

The unobserved natural interest rate depends in turn on two unobserved processes,

$$r_t^* = 4cg_t + z_t, \quad (5)$$

where $4g_t$ is the annualized growth rate of the economy, and z_t captures all the other determinants of r_t^* unrelated to growth.

The three unobserved processes evolve according to

$$y_t^* = y_{t-1}^* + g_{t-1} + \varepsilon_t^{y^*}, \quad (6)$$

$$g_t = g_{t-1} + \varepsilon_t^{g}, \quad (7)$$

$$z_t = z_{t-1} + \varepsilon_t^{z}. \quad (8)$$

The first equation defines the law of motion of potential output, which depends on its past lag and the lagged trend growth rate of the economy. In turn, the second and third equations state that both the trend growth rate of the economy and the z_t component follow random walk processes. Finally, $\varepsilon_t^{y^*}$, ε_t^{g}, and ε_t^{z} are three serially and mutually uncorrelated innovations with variances $\sigma_{y^*}^2$, σ_g^2, and σ_z^2, respectively.

The specific changes introduced in HLW23 are:

1. $\sigma^2_{\tilde{y}}$ and σ^2_{π} are simultaneously scaled up by κ_{2020}, κ_{2021} and κ_{2022} during the last three quarters of 2020, and the whole of 2021 and 2022, respectively, and

2. $\tilde{y}^{adj}_t = \tilde{y}_t + \phi d_t/100$, where d_t is a stringency index of the government responses to the pandemic.

The first adjustment insulates the estimates of r^*_t from the massive outliers observed in real GDP growth during the COVID-19 pandemic. The second adjustment effectively allows for serially correlated but temporary supply shocks resulting from government interventions.

3 Unobservability in the HLW model

3.1 Filter and parameter uncertainty

In state-space models, the mean squared error in the reported estimates of the latent process can be conveniently decomposed into two additive components:

1. Filter uncertainty, which reflects the fact that unless the system is dynamically singular,[1] the state variables cannot be recovered without error from the past, present and future values of the observed variables alone even if one knew the true values of the model parameters.

2. Parameter uncertainty, which reflects the estimation error in those parameters.

Parameter uncertainty will be bounded as long as the model is point identified. In that case, it vanishes as the sample size increases whether one uses frequentists or Bayesian estimation methods thanks to the Bernstein–von Mises theorem.

For the filter uncertainty to be bounded, though, the dynamic system has to be "observable", a concept introduced in Kalman (1960). To define it formally, consider the time-invariant linear system

$$\mathbf{y}_t = \mathbf{C}\mathbf{x}_{t-1} + \mathbf{D}\mathbf{w}_t + \mathbf{u}_t, \tag{9}$$

$$\mathbf{x}_t = \mathbf{A}\mathbf{x}_{t-1} + \mathbf{v}_t, \tag{10}$$

[1] A dynamically singular state-space system is one in which the joint spectral density matrix of the observed and state variables

$$h(\lambda) = \begin{bmatrix} h_{yy}(\lambda) & h^*_{xy}(\lambda) \\ h_{xy}(\lambda) & h_{xx}(\lambda) \end{bmatrix}$$

is such that

$$\int_{-\pi}^{\pi} [h_{xx}(\lambda) - h_{xy}(\lambda) h^{-1}_{yy}(\lambda) h^*_{xy}(\lambda)] d\lambda$$

is singular, where $h^*_{xy}(\lambda)$ is the complex conjugate transpose of $h_{xy}(\lambda)$ (see Proposition 1 in Demos and Sentana (2000) for a univariate version of this result). A trivial example would be a univariate MA(1) process, whose underlying shocks can be recovered without error from the entire path of the observations regardless of whether the MA coefficient is inside, on, or outside the unit interval.

where $\mathbf{w}_t$ is a vector of predetermined observed variables and $dim(\mathbf{x}_t) = s$. Suppose the values of all the system matrices are known, as well as the realisations of the serially and mutually uncorrelated disturbances $\mathbf{u}_t$ and $\mathbf{v}_t$, whose covariance matrices are $\mathbf{R}$ and $\mathbf{Q}$, respectively. Can one learn the initial vector of the unobserved states $\mathbf{x}_0$ by using the history of the observables $\mathbf{y}_t$ and $\mathbf{w}_t$ and those disturbances for $t \geq 1$? In this respect, note that if the answer were negative, one could not recover either the values of the state variables at any subsequent period using the transition equation (10) even in those ideal circumstances.

Most empirical researchers proceed as if the answer to this question were always affirmative. Nevertheless, a necessary and sufficient condition for the time-invariant linear system above to be observable is that the *observability matrix*

$$\mathbf{O} \equiv \begin{pmatrix} \mathbf{C} \\ \mathbf{CA} \\ \mathbf{CA}^2 \\ \vdots \\ \mathbf{CA}^{s-1} \end{pmatrix}, \tag{11}$$

which contains the (impulse) responses of the observed variables to the state variables' shocks, has (column) rank equal to the number of unobserved state variables, and therefore full; see for example Harvey (1989) and Appendix E. Importantly, the matrix $\mathbf{D}$ associated to the coefficients of the observed predetermined variables does not affect the matrix $\mathbf{O}$ in (11) or indeed the observability properties of the system.

3.2 The observability matrix of the HLW model

For pedagogical purposes, consider the following state-space representation of a version of HLW23 with only one lag,[2] in which the measurement equation is given by

$$\begin{aligned} \begin{pmatrix} y_t \\ \pi_t \end{pmatrix} &= \underbrace{\begin{pmatrix} 1-\alpha_y & 1+4c\gamma & \gamma \\ -\kappa & 0 & 0 \end{pmatrix}}_{\mathbf{C}} \begin{pmatrix} y^*_{t-1} \\ g_{t-1} \\ z_{t-1} \end{pmatrix} \\ &+ \underbrace{\begin{pmatrix} \alpha_y & 0 & 0 & -\gamma \\ \kappa & \alpha_\pi & 1-\alpha_\pi & 0 \end{pmatrix}}_{\mathbf{D}} \begin{pmatrix} y_{t-1} \\ \pi_{t-1} \\ \pi_{t-2|4} \\ r_{t-1} \end{pmatrix} + \begin{pmatrix} \varepsilon^{\tilde{y}}_t + \varepsilon^{y^*}_t \\ \varepsilon^{\pi}_t \end{pmatrix}, \end{aligned} \tag{12}$$

[2] By having just one lag of the output gap, we are able to obtain a minimal state space representation of the model with only three unobserved states. Nevertheless, in Appendix A we discuss the observability of the full HLW model, which leads to the same conclusions.

and the transition equation by

$$\begin{pmatrix} y_t^* \\ g_t \\ z_t \end{pmatrix} = \underbrace{\begin{pmatrix} 1 & 1 & 0 \\ 0 & 1 & 0 \\ 0 & 0 & 1 \end{pmatrix}}_{\mathbf{A}} \begin{pmatrix} y_{t-1}^* \\ g_{t-1} \\ z_{t-1} \end{pmatrix} + \begin{pmatrix} \varepsilon_t^{y^*} \\ \varepsilon_t^g \\ \varepsilon_t^z \end{pmatrix}.$$

Given that there are effectively three latent processes, y_t^*, g_t and z_t, but only two observed variables, y_t and π_t,[3] the observability matrix is

$$\mathbf{O} = \begin{pmatrix} \mathbf{C} \\ \mathbf{CA} \\ \mathbf{CA}^2 \end{pmatrix} = \begin{pmatrix} 1-\alpha_y & 1+4c\gamma & \gamma \\ -\kappa & 0 & 0 \\ 1-\alpha_y & 2+4c\gamma-\alpha_y & \gamma \\ -\kappa & -\kappa & 0 \\ 1-\alpha_y & 3+4c\gamma-2\alpha_y & \gamma \\ -\kappa & -2\kappa & 0 \end{pmatrix}, \tag{13}$$

which depends on the following three model parameters:

1. the coefficient of the lagged output gap in the IS curve, α_y;
2. the sensitivity of inflation to the past output gap, κ; and
3. the sensitivity of the output gap to the lagged real rate gap, γ.

By inspecting (13), we can immediately find two important instances of rank deficiency of the observability matrix:

Case 1. The IS curve is flat ($\gamma = 0$)

If the elasticity of the current output gap to the past real interest rate gap is zero, then the IS curve is flat. In that case, the observability matrix becomes

$$\mathbf{O} = \begin{pmatrix} 1-\alpha_y & 1 & 0 \\ -\kappa & 0 & 0 \\ 1-\alpha_y & 2-\alpha_y & 0 \\ -\kappa & -\kappa & 0 \\ 1-\alpha_y & 3-2\alpha_y & 0 \\ -\kappa & -2\kappa & 0 \end{pmatrix},$$

so that the column associated to the z_t process reduces to a vector of zeros. Since the output gap is insensitive to the real interest rate gap, $\tilde{y}_t$ does not provide information about z_t, which contains the non-growth determinants of the natural interest rate. In contrast, one can generally "observe" both potential output y_t^* and its trend-growth component g_t, as long as either the Phillips curve is not flat ($\kappa \neq 0$) or the output gap is covariance stationary ($\alpha_y < 1$).

[3]This state space representation minimizes the length of the state vector but introduces some non-zero correlation across the disturbances of the measurement and state equations, $\mathbf{u}_t$ and $\mathbf{v}_t$. Nevertheless, the specific choice of state space representation does not change results in terms of observability of the full HLW model, as shown in Appendix A. For estimation purposes, though, we employ a different state space representation that exploits the lack of correlation between the disturbances $\mathbf{u}_t$ and $\mathbf{v}_t$; see Appendix B for details.

Case 2. The Phillips curve is flat ($\kappa = 0$)

If the elasticity of current inflation to the past output gap is zero, the Phillips curve is flat. As a result,

$$\mathbf{O} = \begin{pmatrix} 1-\alpha_y & 1+4c\gamma & \gamma \\ 0 & 0 & 0 \\ 1-\alpha_y & 2+4c\gamma-\alpha_y & \gamma \\ 0 & 0 & 0 \\ 1-\alpha_y & 3+4c\gamma-2\alpha_y & \gamma \\ 0 & 0 & 0 \end{pmatrix}.$$

Given that the first and third columns of the observability matrix are proportional, it is not possible to separate potential output y_t^* from the z_t component, while it is still possible to "observe" the process for the underlying trend growth g_t provided the output gap is mean-reverting ($\alpha_y < 1$).[4]

Arguably, these two cases are extreme, but a continuity argument suggests that the filter uncertainty of the HLW model crucially depends on the flatness of the IS and Phillips curves. To verify this conjecture, Figure 1 reports the mean squared errors of the unobserved states as a function of γ and κ using the parameter estimates reported in section 3.3 below. Filter uncertainty associated to the natural interest rate is small for large values of γ and κ. However, when either γ or κ approaches zero, the uncertainty associated with r^* dramatically increases, mostly because of the rise in the uncertainty associated to the z_t component.

3.3 Empirical evidence

In the previous section, we have seen that filter uncertainty about z_t becomes unbounded in the limiting cases of $\gamma = 0$ or $\kappa = 0$, and that it can be very large when any of these parameters is small. But are these values empirically relevant?

Table 1 reports the estimates of γ and κ across several studies that estimate the LW model or some of its variants using data for several advanced economies. As can be seen, typically the estimated sensitivities are statistically significantly different from 0 but very small, so very flat IS and Phillips curves seem to be more the rule than the exception. In this respect, it is important to emphasize that what matters for the observability of r_t^* is the values of those parameters, not their t-ratios.

To assess the extent to which the potential observability difficulties that we have highlighted the HLW23 model may suffer from affect the estimates of the U.S. natural rate posted on the NY Fed web page, we reestimate it using U.S. quarterly data over the period 1960Q3-2025Q1. The first column of Table 2 contains the estimates we obtain using the same procedure as in

[4] Otherwise, y_t^* would not be observable, while one could not tell apart g_t and z_t unless $\gamma = 0$ too.

Table 1: Slopes of IS and Phillips curves: estimates in the literature

		Output gap sensitivity to interest rate gap ($-\gamma$)	Inflation sensitivity to output gap (κ)
United States	Laubach and Williams (2003)	-0.098	0.043
	Clark and Kozicki (2005)	-0.105	0.200
	Trehan and Wu (2007)	-0.130	0.260
	Garnier and Wilhelmsen (2009)	-0.180	0.103
	Kiley (2015)	-0.076	0.073
	Pescatori and Turunen (2015)	-0.060	0.150
	Holston et al. (2017)	-0.071	0.079
	Wynne and Zhang (2017)	-0.107	0.035
	Juselius et al. (2018)	-0.037	0.015
	Buncic (2021)	-0.075	0.081
	Berger et al. (2023)	-0.06	0.18
	Pál and Storti (2025)	-0.054	0.080
Euro area	Mésonnier and Renne (2007)	-0.190	0.160
	Garnier and Wilhelmsen (2009)	-0.056	0.051
	Holston et al. (2017)	-0.036	0.065
	Carvalho (2023)	-0.05	0.06
Canada	Berger and Kempa (2014)	-0.030	0.220
	Holston et al. (2017)	-0.067	0.044
Brazil	Maka (2023)	- 0.038	0.05
Denmark	Pedersen (2015)	-0.400	0.010
Germany	Garnier and Wilhelmsen (2009)	-0.172	0.041
Korea	Suzuki (2020)	-0.254	0.025
Japan	Wynne and Zhang (2017)	-0.043	0.532
South Africa	Kuhn et al. (2017)	-0.032	0.235
Taiwan	Suzuki (2020)	-0.198	0.025
Thailand	Suzuki (2020)	-0.056	0.373
United Kingdom	Holston et al. (2017)	-0.009	0.490
World	Wynne and Zhang (2018)	-0.035	0.159

Notes: In Kiley (2015), κ measures the sensitivity of inflation to an unemployment gap.

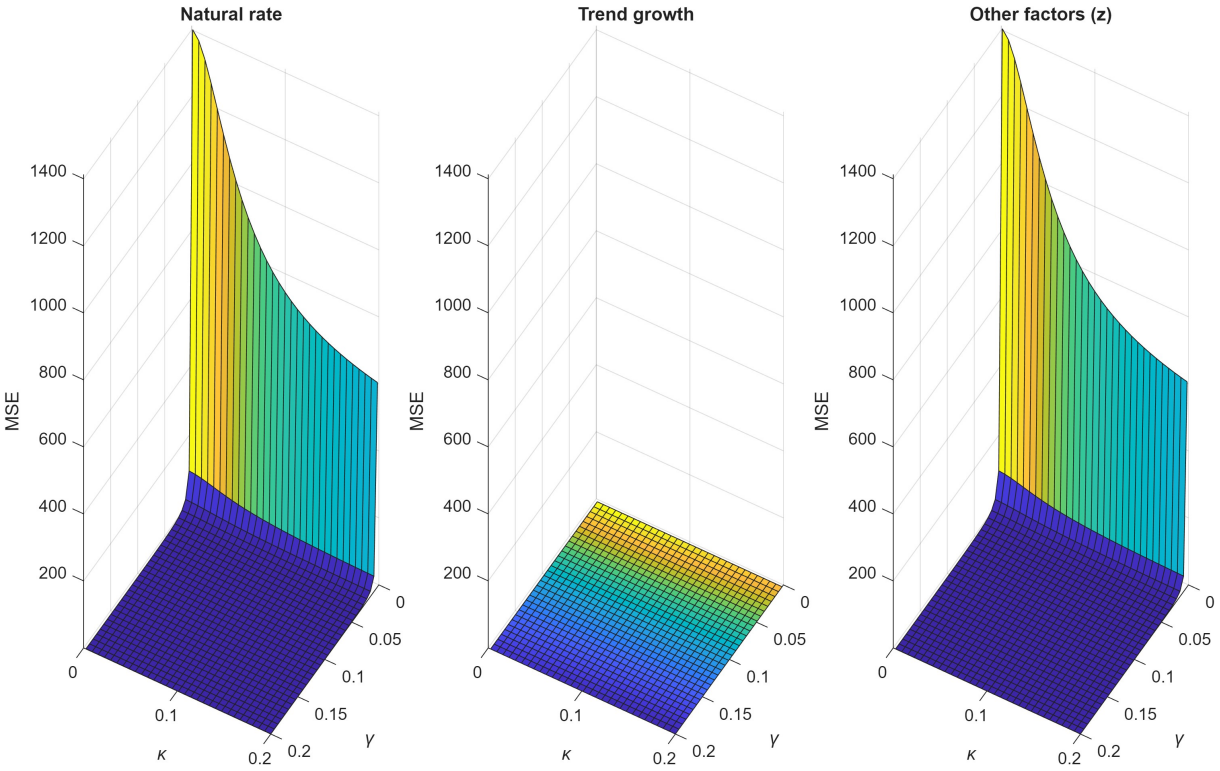

Figure 1: Filter uncertainty in the HLW23 model

that paper. Consistent with the previous literature, we find that the estimates of γ and κ are small (0.071 and 0.076, respectively) but statistically significant.[5]

On the basis of those parameter estimates, Figure 2 displays the (one-sided) filtered values of r_t^* that use information up to and including time t, together with their 68 and 95% confidence bands, which we compute using Hamilton's (1986) Monte Carlo procedure that accounts for both filter and parameter uncertainty, whose details we also provide in Appendix D.[6] As can be seen, the natural rate has declined over time. Nevertheless, it is estimated with little precision, as already emphasized by LW and more recent studies.[7]

In this context, a relevant question is why the uncertainty about r^* is so large. In principle, such imprecise estimates could be due to either *parameter uncertainty*, because the unknown true values of the parameters are estimated with sampling error, or *filter uncertainty*, because the realizations of the state vector are also unknown. To quantify the relative importance of uncertainty on the filter and the parameters, we use the procedures in Appendix D to isolate the role of filter uncertainty by recomputing the bands without accounting for parameter uncertainty

[5]Interestingly, the roots of the AR(2) polynomial in equation (1) are 0.856 and 0.549, which lie well within the unit circle, so that the output gap would be covariance stationary if the interest rate gap were mean-reverting, something which the model is silent about.

[6]See Appendix D.1 for the differences in the computation of the confidence bands between HLW23 and this paper.

[7]See for instance Clark and Kozicki (2005), Kiley (2015), Beyer and Wieland (2019), Lewis and Vazquez-Grande (2019), HLW17 and HLW23.

Table 2: Comparison of Stage 3 Model Estimates

Parameter	Baseline	Augmented
$\alpha_{y,1}$	1.406 (0.103)	1.404 (0.102)
$\alpha_{y,2}$	-0.470 (0.106)	-0.467 (0.103)
γ	0.071 (0.017)	0.076 (0.018)
α_{π}	0.692 (0.040)	0.694 (0.041)
κ	0.073 (0.025)	0.072 (0.025)
$\sigma_{\tilde{y}}$	0.443 (0.095)	0.448 (0.094)
σ_{π}	0.793 (0.027)	0.793 (0.026)
σ_{y^*}	0.497 (0.080)	0.495 (0.078)
ϕ	-0.111 (0.039)	-0.111 (0.039)
c	1.116 (0.335)	0.830 (0.200)
$\kappa_{2020Q2-Q4}$	7.606 (2.799)	7.550 (2.746)
κ_{2021}	1.593 (0.615)	1.583 (0.602)
κ_{2022}	1.935 (0.853)	1.922 (0.902)
σ_{y^*}	2.028	1.883
σ_{r^*}	1.505	0.959
σ_{g}	0.617	0.614
σ_{z}	1.315	0.898
Root 1 AR(2)	0.856 (0.085)	0.861 (0.078)
Root 2 AR(2)	0.549 (0.168)	0.542 (0.159)
α_{r}		0.921 (0.022)
$\sigma_{\tilde{r}}$		0.945 (0.020)
Log-likelihood	-602.531	-602.553

first, and then repeat the exercise without filter uncertainty to assess the role of parameter uncertainty. We report the results of this exercise in Figures 3a and 3b, which depict parameter and filter uncertainty, respectively. As can be seen, uncertainty stemming from the filter is dramatically larger than parameter uncertainty, which suggests that filter uncertainty is the main reason behind the imprecise estimation of the natural rate. Given the results in section 3.2 and Appendix A, this is not at all surprising in view of the small estimates of γ and κ in the first column of Table 2.

Figures 3c and 3d, which depict the evolution of g_t and z_t, respectively, confirm that the main problem is not the filtering of the trend-growth component of r_t^* but rather, of its other determinants, which is in line with the theoretical discussion in section 3.2.

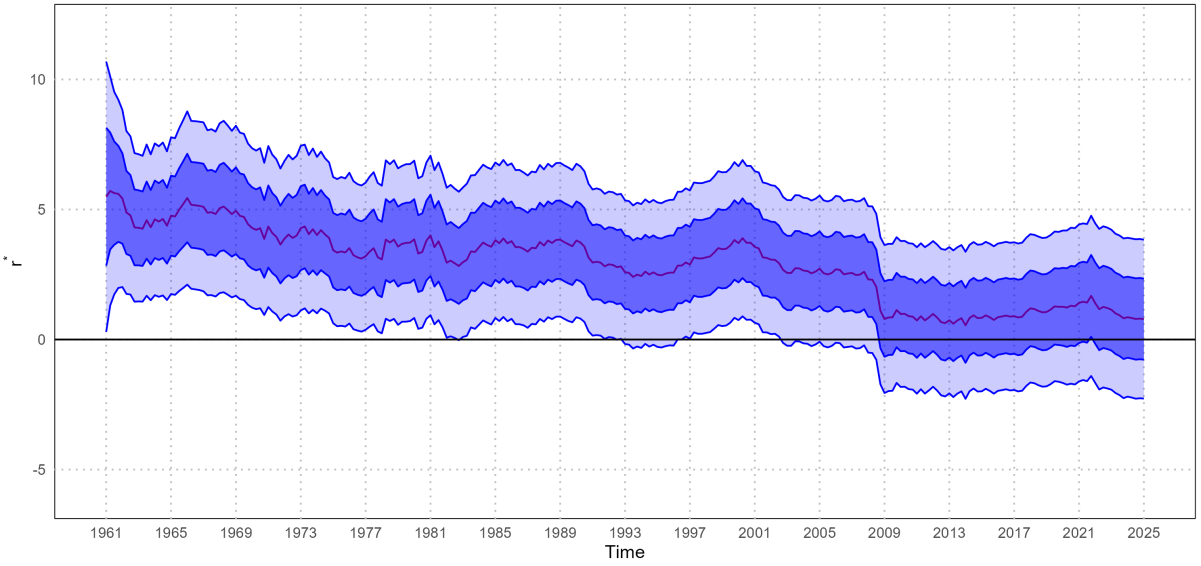

Figure 2: Natural rate of interest in the HLW23 model

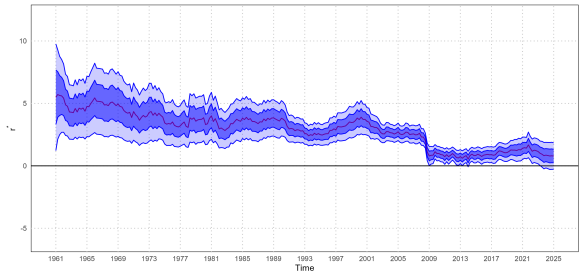

(a) Parameter uncertainty

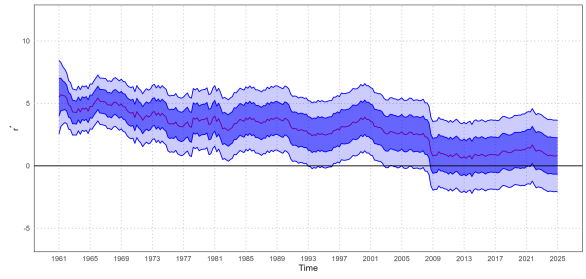

(b) Filter uncertainty

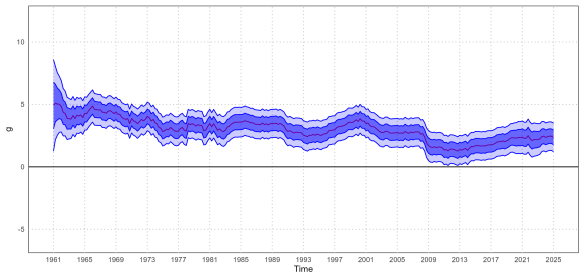

(c) Trend growth g_t

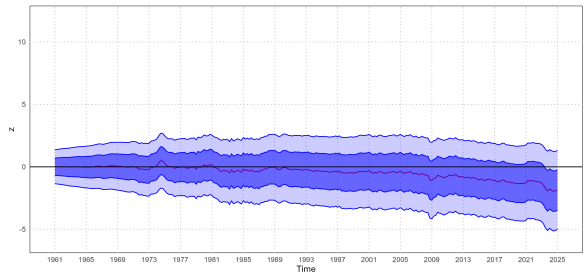

(d) Other determinants z_t

Figure 3: HLW23 model: uncertainty and components of the natural rate r_t^*.

So in summary, the natural interest rate of the HLW model is very imprecisely estimated, mainly because one of its components, the z_t process, is imprecisely estimated too.

4 Achieving observability

4.1 The augmented model

We have previously shown that the HLW model imprecisely estimates the natural interest rate when the IS and the Phillips curves are close to being flat because the z_t component is close to being unobservable in those circumstances. How could one precisely estimate r^* then? To answer this question, we start from the observation that the real interest rate, r_t, only appears in the state-space representation of the HLW model in (12) as an exogenous variable in the transition equation, even though it is crucial in defining the interest rate gap that enters the IS equation (1). This is a direct consequence of the fact that the model leaves the dynamic properties of the interest rate gap itself completely unspecified. In particular, the HLW23 model has no way of guaranteing that the difference between the observed and natural interest rates is mean-reverting. In contrast, it allows for the stationarity of the output gap provided that (i) the autoregressive coefficients $\alpha_{y,1}$ and $\alpha_{y,2}$ that appear in (1) satisfy the usual conditions, and (ii) $\tilde{r}_t$ is indeed stationary; see footnote 5.

As is well known, $\tilde{r}_t$ summarises the stance of monetary policy relative to fundamentals. When $\tilde{r}_t > 0$, the actual real rate is above its natural counterpart and policy is contractionary. In contrast, when $\tilde{r}_t < 0$, policy is expansionary. It is precisely this gap —rather than the level of r_t or r_t^* separately— that drives cyclical fluctuations in the output gap in the aggregate demand relationship (1). Given this interpretation, our modelling choice is to treat $\tilde{r}_t$ as a purely cyclical object by imposing that it is covariance-stationary, so that monetary policy cannot be a source of an additional stochastic trend in the long-run real rate.

This assumption has a clear economic interpretation. In a New Keynesian environment with a Ramsey-type definition of the natural rate, the long-run real interest rate is pinned down by the balanced-growth path of the economy. Monetary policy is typically described by a Taylor-type rule with constant coefficients and an anchored inflation target. Under this rule, persistent drifts in the long-run real rate due to policy simply cannot happen because policy shocks are transitory deviations around a stable reaction function, not an independent source of permanent shifts in r_t^*. More generally, it is difficult to imagine that the U.S. monetary authorities would allow the actual interest rate to diverge from the natural one in the long-run.

By placing the restriction on $\tilde{r}_t$ rather than on the individual components of r_t^*, our approach complements Laubach and Williams (2003), whose focus is the decomposition of the natural rate into the two permanent components that appear in (5). Thus, any low-frequency movements in the long-run real rate are still attributed to r_t^* in our augmented model, while the policy stance $\tilde{r}_t$ remains purely cyclical and stationary. This has two advantages. First, it is consistent with

the idea that monetary policy generates temporary deviations from the balanced-growth path of the economy, but it does not alter this path. Second, it improves the observability of the system, as we explain next.

4.2 Observability in the augmented model

In what follows, we explore the observability properties of an augmented version of the HLW23 model that explicitly allows the interest rate gap to be mean-reverting. For simplicity of exposition, imagine that the interest rate gap follows the covariance stationary AR(1) process

$$\tilde{r}_t = \alpha_r \tilde{r}_{t-1} + \varepsilon_t^{\tilde{r}}, \tag{14}$$

with $|\alpha_r| < 1$, and $\varepsilon_t^{\tilde{r}}$ is a white-noise disturbance, uncorrelated with the other shocks of the model, whose variance is $\sigma_{\tilde{r}}^2$.

To write this augmented model in state-space form, we need to add r_t as an additional left-hand side variable in the measurement equation. Specifically,

$$\begin{pmatrix} y_t \\ \pi_t \\ r_t \end{pmatrix} = \underbrace{\begin{bmatrix} 1-\alpha_y & 1+4\gamma & \gamma \\ -\kappa & 0 & 0 \\ 0 & 4(1-\alpha_r) & 1-\alpha_r \end{bmatrix}}_{\mathbf{C}} \begin{pmatrix} y_{t-1}^* \\ g_{t-1} \\ z_{t-1} \end{pmatrix} + \\ + \underbrace{\begin{pmatrix} \alpha_y & 0 & 0 & -\gamma \\ \kappa & \alpha_\pi & 1-\alpha_\pi & 0 \\ 0 & 0 & 0 & \alpha_r \end{pmatrix}}_{\mathbf{D}} \begin{pmatrix} y_{t-1} \\ \pi_{t-1} \\ \pi_{t-2|4} \\ r_{t-1} \end{pmatrix} + \begin{pmatrix} \varepsilon_t^{\tilde{y}} + \varepsilon_t^{y^*} \\ \varepsilon_t^{\pi} \\ 4\varepsilon_t^{g} + \varepsilon_t^{z} + \varepsilon_t^{\tilde{r}} \end{pmatrix},$$

where, once again we have assumed for simplicity that only one lag of the output gap enters the right-hand side of the IS curve (1) (see Appendix A for the general case). The key difference with respect to the original HLW23 model is that the observed real rate is now an output of the model, as it depends on the three unobserved state variables through the **C** matrix. In contrast, the transition equation is essentially unchanged with respect to the standard HLW model, being given by

$$\begin{pmatrix} y_t^* \\ g_t \\ z_t \end{pmatrix} = \underbrace{\begin{pmatrix} 1 & 1 & 0 \\ 0 & 1 & 0 \\ 0 & 0 & 1 \end{pmatrix}}_{\mathbf{A}} \begin{pmatrix} y_{t-1}^* \\ g_{t-1} \\ z_{t-1} \end{pmatrix} + \begin{pmatrix} \varepsilon_t^{y^*} \\ \varepsilon_t^{g} \\ \varepsilon_t^{z} \end{pmatrix}.$$

The observability of the augmented HLW model now depends on the rank of the matrix

$$\mathbf{O} = \begin{pmatrix} \mathbf{C} \\ \mathbf{CA} \\ \mathbf{CA}^2 \end{pmatrix} = \begin{bmatrix} 1-\alpha_y & 1+4\gamma & \gamma \\ -\kappa & 0 & 0 \\ 0 & 4(1-\alpha_r) & 1-\alpha_r \\ 1-\alpha_y & 2+4\gamma-\alpha_y & \gamma \\ -\kappa & -\kappa & 0 \\ 0 & 4(1-\alpha_r) & 1-\alpha_r \\ 1-\alpha_y & 3+4\gamma-2\alpha_y & \gamma \\ -\kappa & -2\kappa & 0 \\ 0 & 4(1-\alpha_r) & 1-\alpha_r \end{bmatrix}. \tag{15}$$

Compared to the observability matrix of the original HLW model in (13), this matrix includes three additional rows (third, sixth, and ninth), which also depend on the autoregressive coefficient of the interest rate gap, α_r. Those three rows are nonzero when the interest rate gap is stationary, $|\alpha_r| < 1$, and therefore help identify the unobserved states of the model. To illustrate our claim, suppose that both Phillips and IS curves are flat, so that $\gamma = 0$ and $\kappa = 0$. In this extreme case the observability matrix in (15) becomes

$$\mathbf{O} = \begin{bmatrix} 1-\alpha_y & 1 & 0 \\ 0 & 0 & 0 \\ 0 & 4(1-\alpha_r) & 1-\alpha_r \\ 1-\alpha_y & 2-\alpha_y & 0 \\ 0 & 0 & 0 \\ 0 & 4(1-\alpha_r) & 1-\alpha_r \\ 1-\alpha_y & 3-2\alpha_y & 0 \\ 0 & 0 & 0 \\ 0 & 4(1-\alpha_r) & 1-\alpha_r \end{bmatrix}.$$

Importantly, the third column, which is associated to the z_t process, is a nonzero linearly independent vector when the interest rate gap is stationary, $|\alpha_r| < 1$, so that it would now be possible to recover the entire path for the z_t process. More generally, as long as both the interest rate gap and the output gap are stationary, $\text{Rank}(\mathbf{O}) = 3$, so all unobserved states could be recovered from the data under the ideal circumstances described in section 3.1.[8]

We illustrate the practical implications of our theoretical results in Figure 4, which reports the mean squared error of the unobserved states as a function of γ and κ using the parameter estimates reported in the second column of Table 2. Although filter uncertainty associated to the natural interest rate is large for small values of γ and κ, it remains clearly bounded when these parameters go to 0, unlike what happened with the original HLW23 model in Figure 1.

[8] If the interest rate gap were nonstationary, the process for the observed real interest rate would be the sum of two unobserved nonstationary processes, the natural interest rate and the rate gap, which could not be told apart. In that particular case, the ranks of the observability matrices of the original and augmented models in (13) and (15), respectively, would coincide.

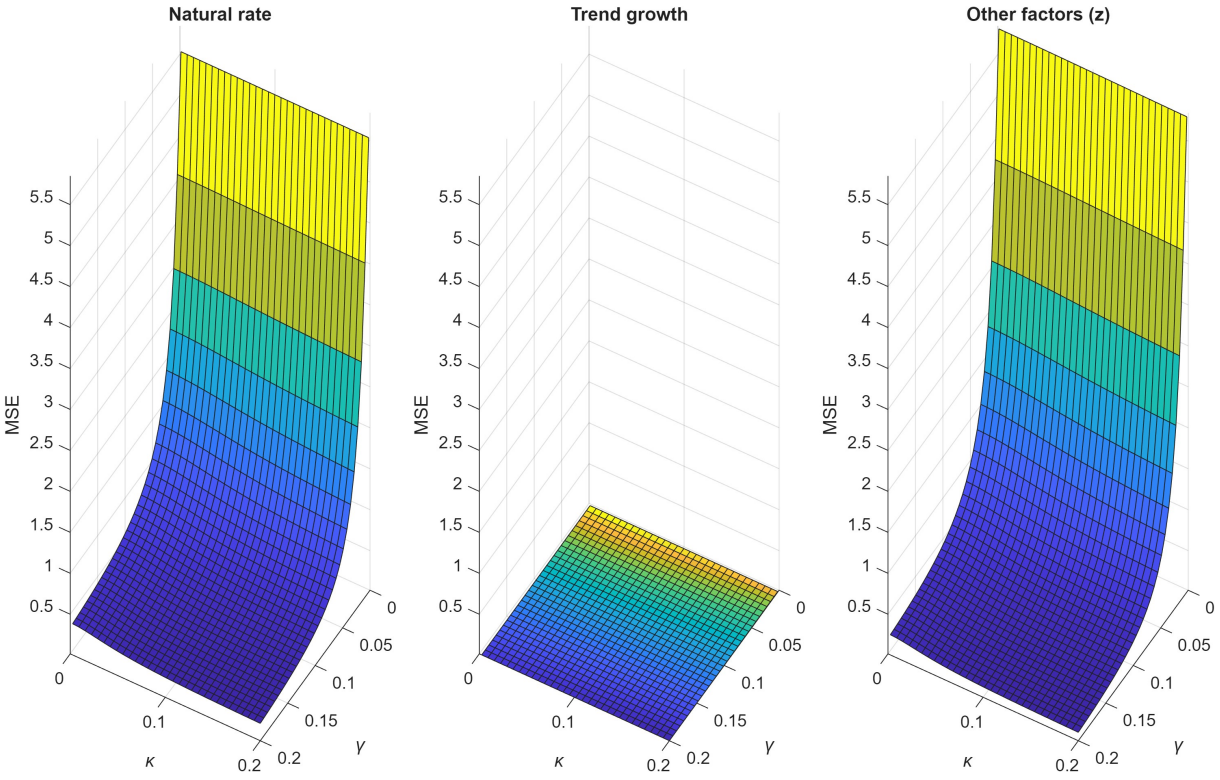

Figure 4: Filter uncertainty in the augmented model

4.3 Empirical evidence

We have estimated the version of the model that adds equation (14) to the HLW23 specification using the procedure described in Appendix B, which is entirely analogous to the procedure used for estimating the original model. The second column of Table 2 contains the parameter estimates thus obtained. Interestingly, for the common parameters, the differences in the MLEs of the original and augmented model are small. This is confirmed by the values of the log-likelihood functions for output and inflation, which are essentially identical (see Appendix C for further details). The estimated persistence of the real interest rate gap, $\alpha_{\tilde{r}}$, is around 0.92, which is high, but its small standard error suggests it is below unity. As we will see below, the persistence of the gap contributes to filter uncertainty, which nevertheless is noticeably lower than in the original model.

Specifically, we use the aforementioned parameter estimates to compute filtered estimates of the different latent variables, as well as confidence bands around them. Once again, we also decompose the bands for the natural rate into filter and parameter uncertainty components. A comparison of Figures 5-6d with Figures 2-3d indicate a considerable reduction in the width of the confidence bands. As expected, most of the gains come from the narrowing of the bands surrounding z_t. In contrast, the median (i.e. central tendency) estimates are rather similar,

although naturally, there are some small differences.

As is well known, the comparison between the observed real rate and the estimated natural rate is often used to characterize the monetary policy stance. Periods in which the gap between those rates is significantly negative are interpreted as episodes of loose monetary policy, while periods in which it is above zero correspond to tightening phases. Figures 7a makes clear that the HLW23 model makes these assessments rather difficult. Aside from the Burns and Volcker eras, and the COVID-19 period, there is hardly any other instance in which the interest rate gap is significantly different from 0. In contrast, Figure 7b shows that the augmented model uncovers some additional episodes of non-neutral policy stances, such as in the period between the end of the dotcom bubble and the global financial crisis, when monetary policy was arguably excessively loose, or after the great recession.

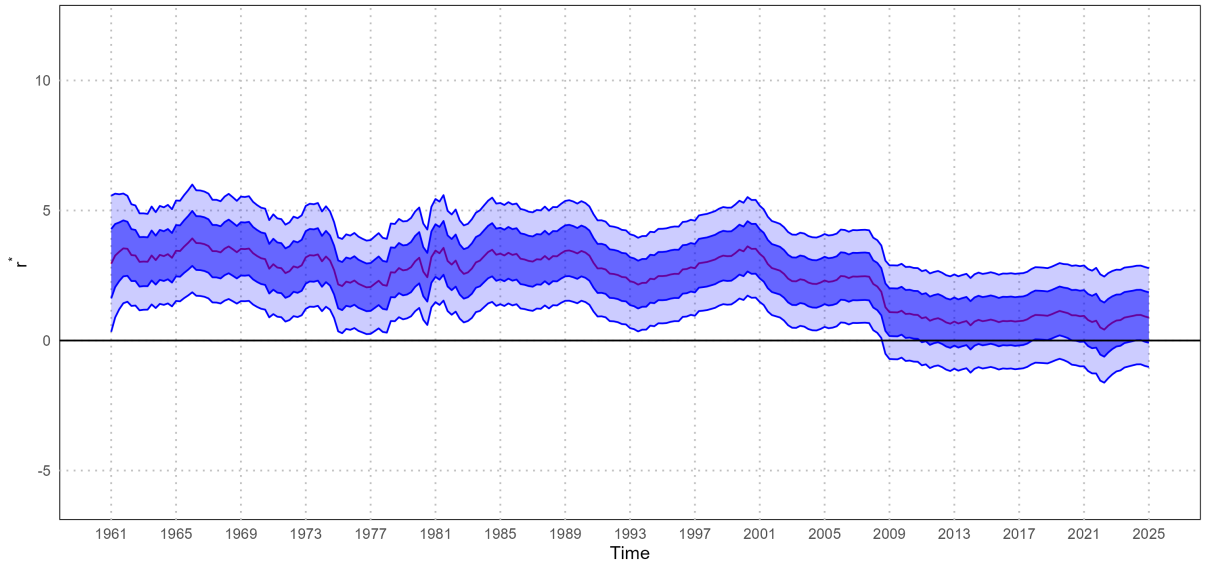

Figure 5: Natural rate of interest in the augmented model

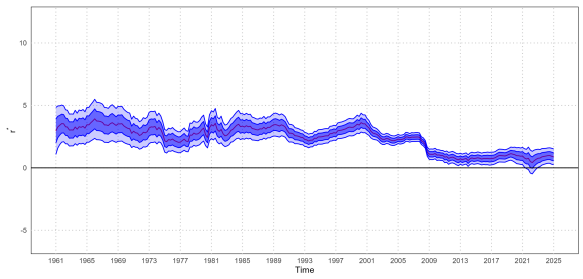

(a) Parameter uncertainty in the augmented model

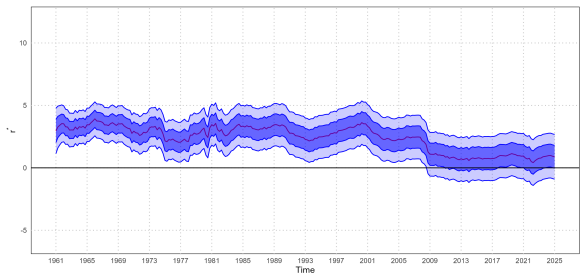

(b) Filter uncertainty in the augmented model

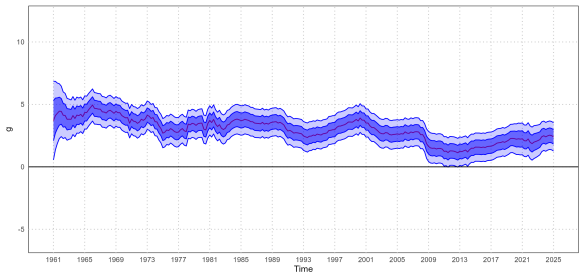

(c) Trend growth component g_t in the augmented model

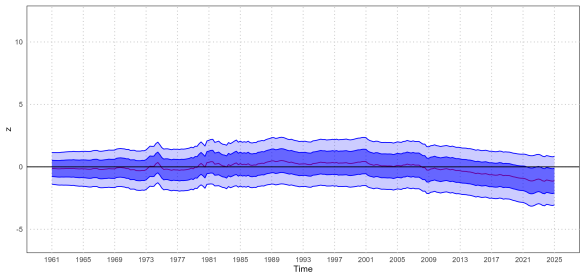

(d) Other determinants z_t in the augmented model

Figure 6: Natural rate of interest in the augmented model: uncertainty and components of r_t^*.

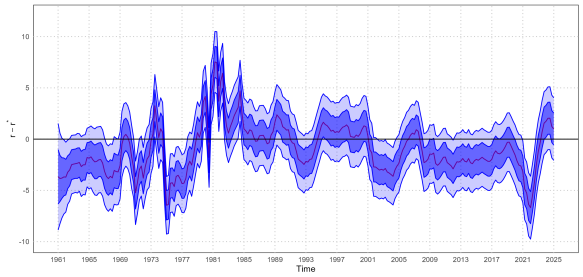

(a) HLW23 model

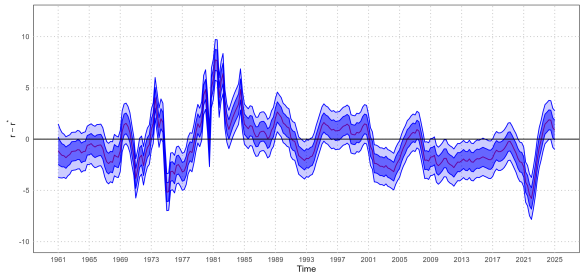

(b) Augmented model

Figure 7: Gap between the real interest rate and the natural rate of interest in the HLW23 and augmented models.

Empirically, the observed ex ante real rate r_t and the estimated natural rate r_t^* display similar low-frequency movements, whereas their difference $\tilde{r}_t$ behaves as a medium-frequency, mean-reverting process. In our estimates, the gap reverts towards its long-run mean at a moderate speed, which is consistent with the idea that systematic monetary policy reacts to deviations from the natural rate and gradually closes them over time. Imposing stationarity of $\tilde{r}_t$ is therefore both theoretically coherent and empirically in line with the observed behaviour of real interest rates.

5 Potential economic determinants of z_t

One potential shortcoming of both the HLW model and our augmented version is that the non-growth composite factor z_t affecting the natural rate of interest is not easily interpretable. To try to remedy this limitation, we explore a version of our augmented model in which

$$z_t = \gamma_z z_{t-1} + \gamma_R Risk_t + \gamma_A Age_t + \varepsilon_t^z, \tag{16}$$

where

1. *Risk* is the corporate risk premium from FRED (BAA10YM),
2. *Age* is a measure of young-age population share, calculated as the ratio of the population aged between 20 and 39 over total population.[9]

The temporal evolution of these series is displayed in Figures 8a and 8b.

When we estimate our augmented model including equation (16), the maximum likelihood estimates (and standard errors) of its parameters are $\gamma_z = 0.529$ (0.096), $\gamma_R = -0.883$ (0.130) and $\gamma_A = 0.070$ (0.024), which have the right signs and are statistically significant.

Unfortunately, as Figure 8c illustrates, they give rise to natural rate estimates that move too much relative to the models that do not include those economic determinants.

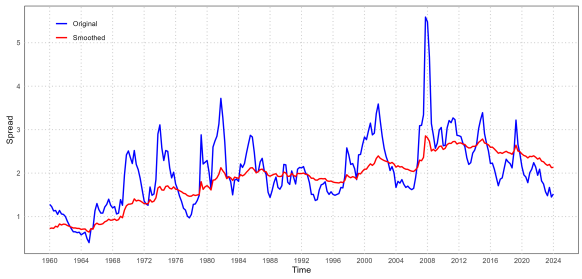

(a) (Smoothed) Corporate risk premium

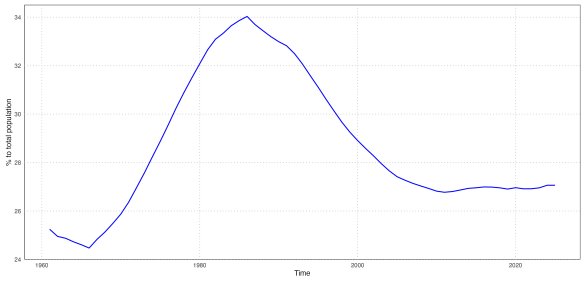

(b) Young-age population share

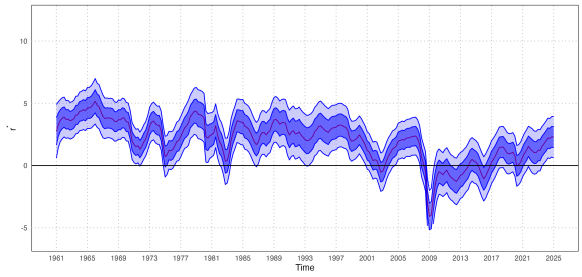

(c) r^* with economic determinants

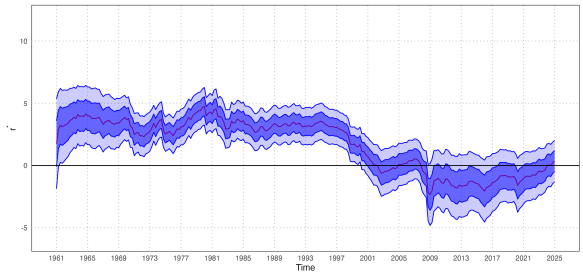

(d) r^* with smoothed economic determinants

Figure 8: Economic determinants of the natural rate of interest and their relationship with r_t^*.

[9]The ratio is available at an annual frequency, and quarterly values are obtained through linear interpolation.

To investigate whether these seemingly excessive movements are the result of the high frequency variation in the corporate risk premium, we have estimated an alternative version with a smoothed version of this risk appetite proxy obtained by assuming a random walk plus noise for it and filtering its transitory component out. Although Figure 8a confirms that the estimated trend in the corporate risk premium is substantially less variable than the original series, Figure 8d shows that the natural rate that we obtain continues to display high frequency variation, with movements that closely follow the behaviour of the real interest rate.

Taken together, this suggests that the mapping between observable slow-moving fundamentals and the latent natural rate may be weaker or more nonlinear than commonly assumed. It also indicates that caution is needed when attempting to ascribe structural interpretations to the latent factors estimated in reduced-form state-space models.

To understand better the empirical failure of equation (16), it is important to emphasise that trend growth in output does not represent trend TFP growth alone. Instead, g_t corresponds to the growth rate of potential output, which in a standard growth-accounting decomposition satisfies

$$g_t = g_t^{TFP} + \alpha\, g_t^K + (1-\alpha)\, g_t^L, \tag{17}$$

where g_t^{TFP} denotes trend TFP growth, g_t^K the trend growth of the capital stock, and g_t^L the trend growth of labour input. While empirically most of the low-frequency variation in g_t tends to be driven by trend TFP, equation (17) makes clear that g_t encompasses all forces that influence the long-run growth rate of potential output.

Specifically, demographic ageing affects g_t primarily through its impact on trend labour input. A decline in the growth rate of the working-age population or a permanent reduction in labour force participation mechanically reduce the trend growth rate of effective labour, lowering the contribution of these variables to potential output growth. In turn, slower labour force growth raises the capital–labour ratio, reducing the marginal product of capital and therefore, investment and capital accumulation. Moreover, ageing also depresses the trend growth of the capital stock through this channel. As a result, demographic ageing lowers g_t not only through labour-input dynamics but also indirectly via reduced capital deepening. Therefore, ageing is naturally embedded in the stochastic trend g_t,

A similar mechanism operates for persistent movements in risk premia. An increase in the risk premium raises the required return on capital, thereby increasing the cost of investment and reducing desired investment rates. Lower investment slows the growth of the capital stock, reducing the contribution of capital accumulation g_t^K to potential output growth. Since trend output growth reflects the contributions of TFP, labour input and capital, a persistent rise in

risk premia depresses g_t by lowering the long-run contribution of capital deepening. Because this is a structural, low-frequency force that alters the balanced-growth path of the economy, it is naturally incorporated into the stochastic trend g_t.

These considerations imply that the stochastic trend g_t in equation (5) already captures the non-stationary structural determinants of the natural rate of interest: trend TFP, demographic forces such as ageing, and persistent movements in risk premia. Therefore, the residual component z_t captures deviations from this balanced-growth path. In this respect, modelling z_t as an explicit function of some of the determinants of the natural rate might imply an identification problem that may explain the poor results that we have obtained when we explore this path.

To further assess whether g_t indeed captures the bulk of the structural determinants highlighted in the literature, we estimate a cointegration relationship between the filtered value of g_t in our augmented model and the three standard long-run drivers of the natural rate: trend productivity growth,[10] demographic dynamics and persistent movements in risk premia. We find strong statistical evidence of cointegration among these variables, with coefficients displaying the expected signs: higher TFP growth raises g_t, while population ageing and an increase in the risk premium reduce it.

The existence of a single cointegrating vector confirms that these three structural forces share a unique common stochastic trend, which is precisely the trend component g_t in our model. This empirical result supports our baseline modelling choice. We interpret g_t as capturing permanent movements in the natural rate that arise from changes in the trend growth rate of potential output, while z_t captures other forces that shift the natural rate independently of long-run growth. Factors such as demographic ageing or changes in risk premia may influence the natural rate both directly and indirectly through their effects on trend growth. Because these channels are difficult to disentangle empirically, including them separately in the model seems to create identification problems.

6 Conclusions

The natural rate of interest remains a central but elusive concept in monetary policy analysis. The widely used Laubach and Williams (2003) framework and its later refinements (Holston, Laubach, and Williams, 2017, 2023) can only identify the natural rate when both the IS and Phillips curves are sufficiently steep. When either aggregate demand or inflation responds weakly—a common empirical case—the model becomes nearly unobservable in the Kalman sense, making the natural rate, and particularly its non-growth component, estimated with extreme

[10] To compute $\Delta \log(\text{TFP}_t)$, we first obtain quarterly values of TFP by linearly interpolating the annual series for Total Factor Productivity for the private business sector compiled by the U.S. Bureau of Labor Statistics.

imprecision. This explains the wide confidence bands and interpretive ambiguity surrounding HLW-type estimates.

We resolve this problem by imposing covariance stationarity of the real interest rate gap, which effectively assumes monetary policy prevents the observed real rate from drifting permanently away from its natural level. This minimal and economically consistent modification restores observability even under flat IS and Phillips curves. The augmented model delivers natural-rate estimates with similar central tendencies to HLW23 but markedly narrower confidence bands, especially for the non-growth component.

Better identification also sharpens the reading of monetary policy stance: while HLW23 often suggests neutrality, our estimates reveal additional episodes of accommodative and restrictive policy consistent with historical narratives. Finally, although the corporate risk premium and demographic structure are statistically significant in explaining the non-growth component of the natural rate, they imply excessive short-term volatility, highlighting that the link between observable fundamentals and the latent rate is weaker or more nonlinear than typically assumed.

Overall, the imprecision of standard natural-rate estimates arises less from data limitations than from lack of observability in the model itself. A model that allows the real interest rate gap to be mean-reverting resolves this problem while maintaining conceptual continuity with the existing literature. Future research could further investigate alternative sources of low-frequency variation in the natural rate and assess the robustness of our identification result in multi-country or structural DSGE settings.

References

Andrews, D., and W. Ploberger (1994): "Optimal tests when a nuisance parameter is present only under the alternative", *Econometrica* 62, 1383-1414.

Beyer, R. C. M., and V. Wieland (2019): "Instability, imprecision, and inconsistent use of equilibrium real interest rate estimates", *Journal of International Money and Finance* 94, 1-14.

Berger, T. and B. Kempa (2014): "Time-varying equilibrium rates in small open economies: evidence for Canada", *Journal of Macroeconomics* 39, 203-214.

Berger, T., B. Kempa, and F. Zou (2023): "The role of macroeconomic uncertainty in the determination of the natural rate of interest", *Economics Letters* 229.

Buncic, D. (2021): "Econometric issues with Laubach and Williams' estimates of the natural rate of interest", arXiv preprint:2002.11583.

Carvalho, A. (2023): "The euro area natural interest rate – Estimation and importance for monetary policy", *Banco de Portugal Economic Studies* IX(3).

Carvalho, C., A. Ferrero, and F. Nechio (2016): "Demographics and real interest rates: inspecting the mechanism", *European Economic Review* 88, 208-226.

Clark, T.E., and S. Kozicki (2005): "Estimating equilibrium real interest rates in real time", *North American Journal of Economics and Finance* 16, 395-413.

Demos, A. and Sentana, E. (2000): "How does the future change our past views of the present", mimeo, CEMFI.

Fiorentini, G., Galesi, A., Pérez-Quirós, G. and Sentana, E. (2018): "The rise and fall of the natural interest rate", *Banco de España Working Paper* 1819.

Garnier, J., and B-R. Wilhelmsen (2009): "The natural rate of interest and the output gap in the euro area: a joint estimation", *Empirical Economics* 36, 297-319.

Hamilton, J. D. (1986): "A standard error for the estimated state vector of a state-space model", *Journal of Econometrics* 333, 387-397.

Harvey, A. (1989): *Forecasting, structural time series models and the Kalman filter*, Cambridge University Press.

Holston, K., T. Laubach, and J. C. Williams (2017): "Measuring the natural rate of interest: international trends and determinants" *Journal of International Economics* 108, S59-S75.

Holston, K., T. Laubach, and J. C. Williams (2023): "Measuring the natural rate of interest after COVID-19 " *Federal Reserve Bank of New York Staff Reports* 1063.

Human Mortality Database. University of California, Berkeley (USA), and Max Planck Institute for Demographic Research (Germany). Available at www.mortality.org and www.humanmortality.de.

Juselius, M., C. Borio, P. Disyatat, and M. Drehmann (2017): "Monetary policy, the financial cycle, and ultra-low interest rates", *International Journal of Central Banking* 13, 55-89.

Kalman, R. E. (1960): "On the general theory of control systems", Proceedings of the First International Congress on Automatic Control, Moscow.

Kiley, M. (2015): "What can the data tell us about the equilibrium real interest rate?", Board of Governors of the Federal Reserve System *Finance and Economics Discussion Series* 2015-077.

Kuhn, L., F. Ruch, and R. Steinbach (2017): "Reaching for the (r)-stars: estimating South Africa's neutral real interest rate", *SARB Working Papers*.

Kuttner, K. N. (1994): "Estimating potential output as a latent variable", *Journal of Business & Economic Statistics*, 12, 361-368.

Laubach, T. (2001) "Measuring the NAIRU: evidence from seven economies", *Review of Economics and Statistics* 83, 218-231.

Laubach, T., and J. C. Williams (2003): "Measuring the natural rate of interest", *Review of Economics and Statistics* 85, 1063-1070.

Lewis, K. F., and F. Vazquez-Grande (2019): "Measuring the natural rate of interest: a note on transitory shocks", *Journal of Applied Econometrics* 34, 425-436.

Maka, A. (2023): "Measuring the natural rate of interest in Brazil", *Institute for Applied Economic Research Discussion Paper 274.*

Mésonnier, J-S., and J-P. Renne (2007): "A time-varying "natural" rate of interest for the euro area", *European Economic Review* 51, 1768-1784.

Pál, T. and G. Storti (2025): "Estimating the r-star in the US: a score-driven state-space model with time-varying volatility persistence", *MPRA (Munich Personal RePEc Archive) Paper* 125338.

Pedersen, J. (2015) "The Danish natural real rate of interest and secular stagnation", *Danmarks Nationalbank Working Papers* 94.

Pescatori, A. and J. Turunen (2015): "Lower for longer: neutral rates in the United States" *International Monetary Fund Working Paper Series* 135.

Rush, J., Orlik, T. and Flanders, S. (eds.) (2025): *The price of money: a guide to the past, present, and future of the natural interest rate*, Oxford University Press.

Rachel, L. and T. D. Smith (2017): "Are low real interest rates here to stay?", *International Journal of Central Banking* 13, 1-42.

Stock, J. H. (1994): "Unit roots, structural breaks, and trends", in: R., Engle (Ed.), Handbook of Econometrics. Vol. 4, 2739-2841. Elsevier.

Stock, J. H., and M. W. Watson (1998): "Median unbiased estimation of coefficient variance in a time-varying parameter model", *Journal of the American Statistical Association* 93, 349-358.

Suzuki, H. (2020): "Two crises and the natural rate of interest: evidence from Taiwan, Thailand, and Korea", *Southeast Asian journal of economics* 8.

Trehan, B. and T. Wu (2007): "Time-varying equilibrium real rates and monetary policy analysis", *Journal of Economic Dynamics and Control* 31, 1584-1609.

Watson, M. W. (1986): "Univariate detrending with stochastic trends", *Journal of Monetary Economics* 18, 49-75.

Wynne, M. A., and R. Zhang (2017): "Estimating the natural rate of interest in an open economy", *Empirical Economics* 1-28.

Wynne, M. A., and R. Zhang (2018): "Measuring the world natural rate of interest", *Economic Inquiry* 56, 530-544.

A Observability in the HLW model

A.1 The original model

Although it is possible to come up with a minimal state space representation, for the sake of clarity we use the same state-space representation as HLW23, whose measurement equation reads

$$\begin{pmatrix} y_t \\ \pi_t \end{pmatrix} = \begin{pmatrix} 1 & -\alpha_{y,1} & -\alpha_{y,2} & 0 & -2c\gamma & -2c\gamma & 0 & -\gamma/2 & -\gamma/2 & 0 \\ 0 & -\kappa & 0 & 0 & 0 & 0 & 0 & 0 & 0 & 0 \end{pmatrix} \begin{pmatrix} y_t^* \\ y_{t-1}^* \\ y_{t-2}^* \\ g_t \\ g_{t-1} \\ g_{t-2} \\ z_t \\ z_{t-1} \\ z_{t-2} \end{pmatrix}$$

$$+ \begin{pmatrix} \alpha_{y,1} & \alpha_{y,2} & \gamma/2 & \gamma/2 & 0 & 0 & \phi & -\phi\alpha_{y,1} & -\phi\alpha_{y,2} \\ \kappa & 0 & 0 & 0 & \alpha_\pi & 1-\alpha_\pi & 0 & -\phi\kappa & 0 \end{pmatrix} \begin{pmatrix} y_{t-1} \\ y_{t-2} \\ r_{t-1} \\ r_{t-2} \\ \pi_{t-1} \\ \pi_{t-2,4} \\ d_t \\ d_{t-1} \\ d_{t-2} \end{pmatrix} + \begin{pmatrix} \varepsilon_t^y \\ \varepsilon_t^\pi \end{pmatrix}, \quad \text{(A1)}$$

with covariance matrix of the measurement errors

$$\mathbf{R}_t = \kappa_t^2 \begin{pmatrix} \sigma_{\tilde{y}}^2 & 0 \\ 0 & \sigma_\pi^2 \end{pmatrix},$$

while the transition equation is

$$\begin{pmatrix} y_t^* \\ y_{t-1}^* \\ y_{t-2}^* \\ g_t \\ g_{t-1} \\ g_{t-2} \\ z_t \\ z_{t-1} \\ z_{t-2} \end{pmatrix} = \begin{pmatrix} 1 & 0 & 0 & 1 & 0 & 0 & 0 & 0 & 0 \\ 1 & 0 & 0 & 0 & 0 & 0 & 0 & 0 & 0 \\ 0 & 1 & 0 & 0 & 0 & 0 & 0 & 0 & 0 \\ 0 & 0 & 0 & 1 & 0 & 0 & 0 & 0 & 0 \\ 0 & 0 & 0 & 1 & 0 & 0 & 0 & 0 & 0 \\ 0 & 0 & 0 & 0 & 1 & 0 & 0 & 0 & 0 \\ 0 & 0 & 0 & 0 & 0 & 0 & 1 & 0 & 0 \\ 0 & 0 & 0 & 0 & 0 & 0 & 1 & 0 & 0 \\ 0 & 0 & 0 & 0 & 0 & 0 & 0 & 1 & 0 \end{pmatrix} \begin{pmatrix} y_{t-1}^* \\ y_{t-2}^* \\ y_{t-3}^* \\ g_{t-1} \\ g_{t-2} \\ g_{t-3} \\ z_{t-1} \\ z_{t-2} \\ z_{t-3} \end{pmatrix} + \begin{pmatrix} \varepsilon_t^{y^*} \\ 0 \\ 0 \\ \varepsilon_t^g \\ 0 \\ 0 \\ \varepsilon_t^z \\ 0 \\ 0 \end{pmatrix}, \quad \text{(A2)}$$

with innovation covariance matrix

$$\mathbf{Q} = \begin{pmatrix} \sigma_{y^*}^2 & 0 & 0 & 0 & 0 & 0 & 0 & 0 & 0 \\ 0 & 0 & 0 & 0 & 0 & 0 & 0 & 0 & 0 \\ 0 & 0 & 0 & 0 & 0 & 0 & 0 & 0 & 0 \\ 0 & 0 & 0 & \sigma_g^2 & 0 & 0 & 0 & 0 & 0 \\ 0 & 0 & 0 & 0 & 0 & 0 & 0 & 0 & 0 \\ 0 & 0 & 0 & 0 & 0 & 0 & 0 & 0 & 0 \\ 0 & 0 & 0 & 0 & 0 & 0 & \sigma_z^2 & 0 & 0 \\ 0 & 0 & 0 & 0 & 0 & 0 & 0 & 0 & 0 \\ 0 & 0 & 0 & 0 & 0 & 0 & 0 & 0 & 0 \end{pmatrix}.$$

Consequently, the observability matrix will be given by

$$\begin{bmatrix} 1 & -\alpha_{y,1} & -\alpha_{y,2} & 0 & -2c\gamma & -2c\gamma & 0 & -\gamma/2 & -\gamma/2 \\ 0 & -\kappa & 0 & 0 & 0 & 0 & 0 & 0 & 0 \\ 1-\alpha_{y,1} & -\alpha_{y,2} & 0 & 1-2c\gamma & -2c\gamma & 0 & -\gamma/2 & -\gamma/2 & 0 \\ -\kappa & 0 & 0 & 0 & 0 & 0 & 0 & 0 & 0 \\ 1-\alpha_{y,1}-\alpha_{y,2} & 0 & 0 & 2-\alpha_{y,1}-4c\gamma & 0 & 0 & -\gamma & 0 & 0 \\ -\kappa & 0 & 0 & -\kappa & 0 & 0 & 0 & 0 & 0 \\ 1-\alpha_{y,1}-\alpha_{y,2} & 0 & 0 & 3-2\alpha_{y,1}-\alpha_{y,2}-4c\gamma & 0 & 0 & -\gamma & 0 & 0 \\ -\kappa & 0 & 0 & -2\kappa & 0 & 0 & 0 & 0 & 0 \\ 1-\alpha_{y,1}-\alpha_{y,2} & 0 & 0 & 4-3\alpha_{y,1}-2\alpha_{y,2}-4c\gamma & 0 & 0 & -\gamma & 0 & 0 \\ -\kappa & 0 & 0 & -3\kappa & 0 & 0 & 0 & 0 & 0 \\ 1-\alpha_{y,1}-\alpha_{y,2} & 0 & 0 & 5-4\alpha_{y,1}-3\alpha_{y,2}-4c\gamma & 0 & 0 & -\gamma & 0 & 0 \\ -\kappa & 0 & 0 & -4\kappa & 0 & 0 & 0 & 0 & 0 \\ 1-\alpha_{y,1}-\alpha_{y,2} & 0 & 0 & 6-5\alpha_{y,1}-4\alpha_{y,2}-4c\gamma & 0 & 0 & -\gamma & 0 & 0 \\ -\kappa & 0 & 0 & -5\kappa & 0 & 0 & 0 & 0 & 0 \\ 1-\alpha_{y,1}-\alpha_{y,2} & 0 & 0 & 7-6\alpha_{y,1}-5\alpha_{y,2}-4c\gamma & 0 & 0 & -\gamma & 0 & 0 \\ -\kappa & 0 & 0 & -6\kappa & 0 & 0 & 0 & 0 & 0 \\ 1-\alpha_{y,1}-\alpha_{y,2} & 0 & 0 & 8-7\alpha_{y,1}-6\alpha_{y,2}-4c\gamma & 0 & 0 & -\gamma & 0 & 0 \\ -\kappa & 0 & 0 & -7\kappa & 0 & 0 & 0 & 0 & 0 \end{bmatrix}$$

In general, the rank of this matrix is 6 rather than 9 because the third, sixth and ninth columns are proportional to each other and so are the fifth and eigth ones. Those rank deficiencies are not worrisome, though, because they simply reflect the fact that the state space representation contains too many elements, and we could not separately recover the values of g_{-1} and z_{-1} or distinguish between y^*_{-2}, g_{-2} and z_{-2} even if we could observe the mesurement errors ε_t^y and ε_t^π and shocks $\varepsilon_t^{y^*}$, ε_t^g and ε_t^z for $t \geq 1$. Nevertheless, given that we could indeed recover y_0^*, y_{-1}^*, g_0 and z_0, the first-order Markovian nature of g_t and z_t and the second-order Markovian nature of y_t^* implies that we would be able to infer without error the values of y_t^*, g_t and z_t for $t \geq 1$.

When $\gamma = 0$, so that the IS curve is flat, this matrix reduces to

$$\begin{bmatrix}
1 & -\alpha_{y,1} & -\alpha_{y,2} & 0 & 0 & 0 & 0 & 0 & 0 \\
0 & -\kappa & 0 & 0 & 0 & 0 & 0 & 0 & 0 \\
1-\alpha_{y,1} & -\alpha_{y,2} & 0 & 10 & 0 & 0 & 0 & 0 & 0 \\
-\kappa & 0 & 0 & 0 & 0 & 0 & 0 & 0 & 0 \\
1-\alpha_{y,1}-\alpha_{y,2} & 0 & 0 & 2-\alpha_{y,1} & 0 & 0 & 0 & 0 & 0 \\
-\kappa & 0 & 0 & -\kappa & 0 & 0 & 0 & 0 & 0 \\
1-\alpha_{y,1}-\alpha_{y,2} & 0 & 0 & 3-2\alpha_{y,1}-\alpha_{y,2} & 0 & 0 & 0 & 0 & 0 \\
-\kappa & 0 & 0 & -2\kappa & 0 & 0 & 0 & 0 & 0 \\
1-\alpha_{y,1}-\alpha_{y,2} & 0 & 0 & 4-3\alpha_{y,1}-2\alpha_{y,2} & 0 & 0 & 0 & 0 & 0 \\
-\kappa & 0 & 0 & -3\kappa & 0 & 0 & 0 & 0 & 0 \\
1-\alpha_{y,1}-\alpha_{y,2} & 0 & 0 & 5-4\alpha_{y,1}-3\alpha_{y,2} & 0 & 0 & 0 & 0 & 0 \\
-\kappa & 0 & 0 & -4\kappa & 0 & 0 & 0 & 0 & 0 \\
1-\alpha_{y,1}-\alpha_{y,2} & 0 & 0 & 6-5\alpha_{y,1}-4\alpha_{y,2} & 0 & 0 & 0 & 0 & 0 \\
-\kappa & 0 & 0 & -5\kappa & 0 & 0 & 0 & 0 & 0 \\
1-\alpha_{y,1}-\alpha_{y,2} & 0 & 0 & 7-6\alpha_{y,1}-5\alpha_{y,2} & 0 & 0 & 0 & 0 & 0 \\
-\kappa & 0 & 0 & -6\kappa & 0 & 0 & 0 & 0 & 0 \\
1-\alpha_{y,1}-\alpha_{y,2} & 0 & 0 & 8-7\alpha_{y,1}-6\alpha_{y,2} & 0 & 0 & 0 & 0 & 0 \\
-\kappa & 0 & 0 & -7\kappa & 0 & 0 & 0 & 0 & 0
\end{bmatrix},$$

which only has rank 4 at best. Given that the basis of its nullspace is trivially

$$\begin{pmatrix}
0 & 0 & 0 & 0 & 0 \\
0 & 0 & 0 & 0 & 0 \\
0 & 0 & 0 & 0 & 0 \\
0 & 0 & 0 & 0 & 0 \\
1 & 0 & 0 & 0 & 0 \\
0 & 1 & 0 & 0 & 0 \\
0 & 0 & 1 & 0 & 0 \\
0 & 0 & 0 & 1 & 0 \\
0 & 0 & 0 & 0 & 1
\end{pmatrix},$$

the entire process for z_t will be unobservable even if we could observe all measurement errors and shocks for $t \geq 1$.

Similarly, when $\kappa = 0$, so that the Phillips curve is flat, the observability matrix becomes

$$\begin{bmatrix}
1 & -\alpha_{y,1} & -\alpha_{y,2} & 0 & -2c\gamma & -2c\gamma & 0 & -\gamma/2 & -\gamma/2 \\
0 & 0 & 0 & 0 & 0 & 0 & 0 & 0 & 0 \\
1-\alpha_{y,1} & -\alpha_{y,2} & 0 & 1-2c\gamma & -2c\gamma & 0 & -\gamma/2 & -\gamma/2 & 0 \\
0 & 0 & 0 & 0 & 0 & 0 & 0 & 0 & 0 \\
1-\alpha_{y,1}-\alpha_{y,2} & 0 & 0 & 2-\alpha_{y,1}-4c\gamma & 0 & 0 & -\gamma & 0 & 0 \\
0 & 0 & 0 & 0 & 0 & 0 & 0 & 0 & 0 \\
1-\alpha_{y,1}-\alpha_{y,2} & 0 & 0 & 3-2\alpha_{y,1}-\alpha_{y,2}-4c\gamma & 0 & 0 & -\gamma & 0 & 0 \\
0 & 0 & 0 & 0 & 0 & 0 & 0 & 0 & 0 \\
1-\alpha_{y,1}-\alpha_{y,2} & 0 & 0 & 4-3\alpha_{y,1}-2\alpha_{y,2}-4c\gamma & 0 & 0 & -\gamma & 0 & 0 \\
0 & 0 & 0 & 0 & 0 & 0 & 0 & 0 & 0 \\
1-\alpha_{y,1}-\alpha_{y,2} & 0 & 0 & 5-4\alpha_{y,1}-3\alpha_{y,2}-4c\gamma & 0 & 0 & -\gamma & 0 & 0 \\
0 & 0 & 0 & 0 & 0 & 0 & 0 & 0 & 0 \\
1-\alpha_{y,1}-\alpha_{y,2} & 0 & 0 & 6-5\alpha_{y,1}-4\alpha_{y,2}-4c\gamma & 0 & 0 & -\gamma & 0 & 0 \\
0 & 0 & 0 & 0 & 0 & 0 & 0 & 0 & 0 \\
1-\alpha_{y,1}-\alpha_{y,2} & 0 & 0 & 7-6\alpha_{y,1}-5\alpha_{y,2}-4c\gamma & 0 & 0 & -\gamma & 0 & 0 \\
0 & 0 & 0 & 0 & 0 & 0 & 0 & 0 & 0 \\
1-\alpha_{y,1}-\alpha_{y,2} & 0 & 0 & 8-7\alpha_{y,1}-6\alpha_{y,2}-4c\gamma & 0 & 0 & -\gamma & 0 & 0 \\
0 & 0 & 0 & 0 & 0 & 0 & 0 & 0 & 0
\end{bmatrix},$$

which also has rank 4 because in addition to the three singularities mentioned in the general case, we have that the sum of the first three columns is proportional to the sum of the last three ones, and the fifth column can be obtained as a linear combination of the second and third ones. Specifically, the matrix

$$\begin{bmatrix}
0 & 0 & 0 & \gamma & 0 \\
0 & 0 & 0 & \gamma & -2c\gamma\alpha_{y,2} \\
2c\gamma & \gamma/2 & 0 & \gamma & 2c\gamma(\alpha_{y,1}-\alpha_{y,2}) \\
0 & 0 & 0 & 0 & 0 \\
0 & 0 & \gamma/2 & 0 & \alpha_{y,2}^2 \\
-\alpha_{y,2} & 0 & 0 & 0 & 0 \\
0 & 0 & 0 & 1-\alpha_{y,1}-\alpha_{y,2} & 0 \\
0 & 0 & -2c\gamma & 1-\alpha_{y,1}-\alpha_{y,2} & 0 \\
0 & -\alpha_{y,2} & 0 & 1-\alpha_{y,1}-\alpha_{y,2} & 0
\end{bmatrix}$$

will constitute a basis of its nullspace. Consequently, in addition to the presample values mentioned above, we will not be able to tell apart z_t from potential output or trend growth.

A.2 The augmented model

The assumption that the interest rate gap follows an AR(1) model requires the addition of r_t as an additional observed variable and $\tilde{r}_t$ as an additional latent processes. Thus, the

measurement equation becomes

$$\begin{pmatrix} y_t \\ \pi_t \\ r_t \end{pmatrix} = \begin{bmatrix} 1 & -\alpha_{y,1} & -\alpha_{y,2} & 0 & -2c\gamma & -2c\gamma & 0 & -\gamma/2 & -\gamma/2 & 0 \\ 0 & -\kappa & 0 & 0 & 0 & 0 & 0 & 0 & 0 & 0 \\ 0 & 0 & 0 & 4c & 0 & 0 & 1 & 0 & 0 & 1 \end{bmatrix} \begin{pmatrix} y_t^* \\ y_{t-1}^* \\ y_{t-2}^* \\ g_t \\ g_{t-1} \\ g_{t-2} \\ z_t \\ z_{t-1} \\ z_{t-2} \\ \tilde{r}_t \end{pmatrix}$$

$$+ \begin{bmatrix} \alpha_{y,1} & \alpha_{y,2} & \gamma/2 & \gamma/2 & 0 & 0 & \phi & -\phi\alpha_{y,1} & -\phi\alpha_{y,2} \\ \kappa & 0 & 0 & 0 & \alpha_\pi & 1-\alpha_\pi & 0 & -\phi\kappa & 0 \\ 0 & 0 & 0 & 0 & 0 & 0 & 0 & 0 & 0 \end{bmatrix} \begin{pmatrix} y_{t-1} \\ y_{t-2} \\ r_{t-1} \\ r_{t-2} \\ \pi_{t-1} \\ \pi_{t-2,4} \\ d_t \\ d_{t-1} \\ d_{t-2} \end{pmatrix} + \begin{pmatrix} \varepsilon_t^y \\ \varepsilon_t^\pi \\ 0 \end{pmatrix}, \qquad \text{(A3)}$$

with covariance matrix of the measurement errors

$$R_t = \kappa_t^2 \begin{pmatrix} \sigma_y^2 & 0 & 0 \\ 0 & \sigma_\pi^2 & 0 \\ 0 & 0 & 0 \end{pmatrix},$$

while the transition equation is

$$\begin{pmatrix} y_t^* \\ y_{t-1}^* \\ y_{t-2}^* \\ g_t \\ g_{t-1} \\ g_{t-2} \\ z_t \\ z_{t-1} \\ z_{t-2} \\ \tilde{r}_t \end{pmatrix} = \begin{pmatrix} 1 & 0 & 0 & 1 & 0 & 0 & 0 & 0 & 0 & 0 \\ 1 & 0 & 0 & 0 & 0 & 0 & 0 & 0 & 0 & 0 \\ 0 & 1 & 0 & 0 & 0 & 0 & 0 & 0 & 0 & 0 \\ 0 & 0 & 0 & 1 & 0 & 0 & 0 & 0 & 0 & 0 \\ 0 & 0 & 0 & 1 & 0 & 0 & 0 & 0 & 0 & 0 \\ 0 & 0 & 0 & 0 & 1 & 0 & 0 & 0 & 0 & 0 \\ 0 & 0 & 0 & 0 & 0 & 0 & 1 & 0 & 0 & 0 \\ 0 & 0 & 0 & 0 & 0 & 0 & 1 & 0 & 0 & 0 \\ 0 & 0 & 0 & 0 & 0 & 0 & 0 & 1 & 0 & 0 \\ 0 & 0 & 0 & 0 & 0 & 0 & 0 & 0 & 0 & \alpha_r \end{pmatrix} \begin{pmatrix} y_{t-1}^* \\ y_{t-2}^* \\ y_{t-3}^* \\ g_{t-1} \\ g_{t-2} \\ g_{t-3} \\ z_{t-1} \\ z_{t-2} \\ z_{t-3} \\ \tilde{r}_{t-1} \end{pmatrix} + \begin{pmatrix} \varepsilon_t^{y^*} \\ 0 \\ 0 \\ \varepsilon_t^g \\ 0 \\ 0 \\ \varepsilon_t^z \\ 0 \\ 0 \\ \varepsilon_t^{\tilde{r}} \end{pmatrix}, \qquad \text{(A4)}$$

with innovariation covariance matrix

$$\mathbf{Q} = \begin{pmatrix} \sigma_{y^*}^2 & 0 & 0 & 0 & 0 & 0 & 0 & 0 & 0 & 0 \\ 0 & 0 & 0 & 0 & 0 & 0 & 0 & 0 & 0 & 0 \\ 0 & 0 & 0 & 0 & 0 & 0 & 0 & 0 & 0 & 0 \\ 0 & 0 & 0 & \sigma_g^2 & 0 & 0 & 0 & 0 & 0 & 0 \\ 0 & 0 & 0 & 0 & 0 & 0 & 0 & 0 & 0 & 0 \\ 0 & 0 & 0 & 0 & 0 & 0 & 0 & 0 & 0 & 0 \\ 0 & 0 & 0 & 0 & 0 & 0 & \sigma_z^2 & 0 & 0 & 0 \\ 0 & 0 & 0 & 0 & 0 & 0 & 0 & 0 & 0 & 0 \\ 0 & 0 & 0 & 0 & 0 & 0 & 0 & 0 & 0 & 0 \\ 0 & 0 & 0 & 0 & 0 & 0 & 0 & 0 & 0 & \sigma_{\tilde{r}}^2 \end{pmatrix}.$$

Consequently, the observability matrix will be given by

$$\begin{bmatrix} 1 & -\alpha_{y,1} & -\alpha_{y,2} & 0 & -2c\gamma & -2c\gamma & 0 & -\gamma/2 & -\gamma/2 & 0 \\ 0 & -\kappa & 0 & 0 & 0 & 0 & 0 & 0 & 0 & 0 \\ 0 & 0 & 0 & 4c & 0 & 0 & 1 & 0 & 0 & 1 \\ 1-\alpha_{y,1} & -\alpha_{y,2} & 0 & 1-2c\gamma & -2c\gamma & 0 & -\gamma/2 & -\gamma/2 & 0 & 0 \\ -\kappa & 0 & 0 & 0 & 0 & 0 & 0 & 0 & 0 & 0 \\ 0 & 0 & 0 & 4c & 0 & 0 & 1 & 0 & 0 & \alpha_r \\ 1-\alpha_{y,1}-\alpha_{y,2} & 0 & 0 & 2-\alpha_{y,1}-4c\gamma & 0 & 0 & -\gamma & 0 & 0 & 0 \\ -\kappa & 0 & 0 & -\kappa & 0 & 0 & 0 & 0 & 0 & 0 \\ 0 & 0 & 0 & 4c & 0 & 0 & 1 & 0 & 0 & \alpha_r^2 \\ 1-\alpha_{y,1}-\alpha_{y,2} & 0 & 0 & 3-2\alpha_{y,1}-\alpha_{y,2}-4c\gamma & 0 & 0 & -\gamma & 0 & 0 & 0 \\ -\kappa & 0 & 0 & -2\kappa & 0 & 0 & 0 & 0 & 0 & 0 \\ 0 & 0 & 0 & 4c & 0 & 0 & 1 & 0 & 0 & \alpha_r^3 \\ 1-\alpha_{y,1}-\alpha_{y,2} & 0 & 0 & 4-3\alpha_{y,1}-2\alpha_{y,2}-4c\gamma & 0 & 0 & -\gamma & 0 & 0 & 0 \\ -\kappa & 0 & 0 & -3\kappa & 0 & 0 & 0 & 0 & 0 & 0 \\ 0 & 0 & 0 & 4c & 0 & 0 & 1 & 0 & 0 & \alpha_r^4 \\ 1-\alpha_{y,1}-\alpha_{y,2} & 0 & 0 & 5-4\alpha_{y,1}-3\alpha_{y,2}-4c\gamma & 0 & 0 & -\gamma & 0 & 0 & 0 \\ -\kappa & 0 & 0 & -4\kappa & 0 & 0 & 0 & 0 & 0 & 0 \\ 0 & 0 & 0 & 4c & 0 & 0 & 1 & 0 & 0 & \alpha_r^5 \\ 1-\alpha_{y,1}-\alpha_{y,2} & 0 & 0 & 6-5\alpha_{y,1}-4\alpha_{y,2}-4c\gamma & 0 & 0 & -\gamma & 0 & 0 & 0 \\ -\kappa & 0 & 0 & -5\kappa & 0 & 0 & 0 & 0 & 0 & 0 \\ 0 & 0 & 0 & 4c & 0 & 0 & 1 & 0 & 0 & \alpha_r^6 \\ 1-\alpha_{y,1}-\alpha_{y,2} & 0 & 0 & 7-6\alpha_{y,1}-5\alpha_{y,2}-4c\gamma & 0 & 0 & -\gamma & 0 & 0 & 0 \\ -\kappa & 0 & 0 & -6\kappa & 0 & 0 & 0 & 0 & 0 & 0 \\ 0 & 0 & 0 & 4c & 0 & 0 & 1 & 0 & 0 & \alpha_r^7 \\ 1-\alpha_{y,1}-\alpha_{y,2} & 0 & 0 & 8-7\alpha_{y,1}-6\alpha_{y,2}-4c\gamma & 0 & 0 & -\gamma & 0 & 0 & 0 \\ -\kappa & 0 & 0 & -7\kappa & 0 & 0 & 0 & 0 & 0 & 0 \\ 0 & 0 & 0 & 4c & 0 & 0 & 1 & 0 & 0 & \alpha_r^8 \\ 1-\alpha_{y,1}-\alpha_{y,2} & 0 & 0 & 9-8\alpha_{y,1}-7\alpha_{y,2}-4c\gamma & 0 & 0 & -\gamma & 0 & 0 & 0 \\ -\kappa & 0 & 0 & -8\kappa & 0 & 0 & 0 & 0 & 0 & 0 \\ 0 & 0 & 0 & 4c & 0 & 0 & 1 & 0 & 0 & \alpha_r^9 \end{bmatrix},$$

which generally has rank 7 because of the presample observations.

When $\gamma = 0$ and $\kappa = 0$ simultaneously, this matrix becomes

$$\begin{bmatrix}
1 & -\alpha_{y,1} & -\alpha_{y,2} & 0 & 0 & 0 & 0 & 0 & 0 & 0 \\
0 & 0 & 0 & 0 & 0 & 0 & 0 & 0 & 0 & 0 \\
0 & 0 & 0 & 4c & 0 & 0 & 1 & 0 & 0 & 1 \\
1-\alpha_{y,1} & -\alpha_{y,2} & 0 & 1 & 0 & 0 & 0 & 0 & 0 & 0 \\
0 & 0 & 0 & 0 & 0 & 0 & 0 & 0 & 0 & 0 \\
0 & 0 & 0 & 4c & 0 & 0 & 1 & 0 & 0 & \alpha_r \\
1-\alpha_{y,1}-\alpha_{y,2} & 0 & 0 & 2-\alpha_{y,1} & 0 & 0 & 0 & 0 & 0 & 0 \\
0 & 0 & 0 & 0 & 0 & 0 & 0 & 0 & 0 & 0 \\
0 & 0 & 0 & 4c & 0 & 0 & 1 & 0 & 0 & \alpha_r^2 \\
1-\alpha_{y,1}-\alpha_{y,2} & 0 & 0 & 3-2\alpha_{y,1}-\alpha_{y,2} & 0 & 0 & 0 & 0 & 0 & 0 \\
0 & 0 & 0 & 0 & 0 & 0 & 0 & 0 & 0 & 0 \\
0 & 0 & 0 & 4c & 0 & 0 & 1 & 0 & 0 & \alpha_r^3 \\
1-\alpha_{y,1}-\alpha_{y,2} & 0 & 0 & 4-3\alpha_{y,1}-2\alpha_{y,2} & 0 & 0 & 0 & 0 & 0 & 0 \\
0 & 0 & 0 & 0 & 0 & 0 & 0 & 0 & 0 & 0 \\
0 & 0 & 0 & 4c & 0 & 0 & 1 & 0 & 0 & \alpha_r^4 \\
1-\alpha_{y,1}-\alpha_{y,2} & 0 & 0 & 5-4\alpha_{y,1}-3\alpha_{y,2} & 0 & 0 & 0 & 0 & 0 & 0 \\
0 & 0 & 0 & 0 & 0 & 0 & 0 & 0 & 0 & 0 \\
0 & 0 & 0 & 4c & 0 & 0 & 1 & 0 & 0 & \alpha_r^5 \\
1-\alpha_{y,1}-\alpha_{y,2} & 0 & 0 & 6-5\alpha_{y,1}-4\alpha_{y,2} & 0 & 0 & 0 & 0 & 0 & 0 \\
0 & 0 & 0 & 0 & 0 & 0 & 0 & 0 & 0 & 0 \\
0 & 0 & 0 & 4c & 0 & 0 & 1 & 0 & 0 & \alpha_r^6 \\
1-\alpha_{y,1}-\alpha_{y,2} & 0 & 0 & 7-6\alpha_{y,1}-5\alpha_{y,2} & 0 & 0 & 0 & 0 & 0 & 0 \\
0 & 0 & 0 & 0 & 0 & 0 & 0 & 0 & 0 & 0 \\
0 & 0 & 0 & 4c & 0 & 0 & 1 & 0 & 0 & \alpha_r^7 \\
1-\alpha_{y,1}-\alpha_{y,2} & 0 & 0 & 8-7\alpha_{y,1}-6\alpha_{y,2} & 0 & 0 & 0 & 0 & 0 & 0 \\
0 & 0 & 0 & 0 & 0 & 0 & 0 & 0 & 0 & 0 \\
0 & 0 & 0 & 4c & 0 & 0 & 1 & 0 & 0 & \alpha_r^8 \\
1-\alpha_{y,1}-\alpha_{y,2} & 0 & 0 & 9-8\alpha_{y,1}-7\alpha_{y,2} & 0 & 0 & 0 & 0 & 0 & 0 \\
0 & 0 & 0 & 0 & 0 & 0 & 0 & 0 & 0 & 0 \\
0 & 0 & 0 & 4c & 0 & 0 & 1 & 0 & 0 & \alpha_r^9
\end{bmatrix},$$

which has rank 6 provided that $\alpha_r \neq 1$. Nevertheless, given that the basis of its nullspace is

$$\begin{pmatrix}
0 & 0 & 0 & 0 \\
0 & 0 & 0 & 0 \\
0 & 0 & 0 & 0 \\
0 & 0 & 0 & 0 \\
1 & 0 & 0 & 0 \\
0 & 1 & 0 & 0 \\
0 & 0 & 0 & 0 \\
0 & 0 & 1 & 0 \\
0 & 0 & 0 & 1 \\
0 & 0 & 0 & 0
\end{pmatrix},$$

the only consequence of this rank failure is that we could not recover g_{-1}, g_{-2}, z_{-1} and z_{-2} when we observed the values of all the measurement errors and shocks for $t \geq 1$. In contrast, we could recover y^*_{-1}, y^*_{-2}, g_0 and z_0, and consequently all subsequent values of the state variables thanks to the first-order Markovian nature of g_t and z_t and the second-order Markovian nature of y^*_t.

B Estimating the augmented version of the HLW model

As we have seen in Appendix A, the different versions of the LW model can be cast in state-space form, which allows the use of the standard Kalman filter to estimate its parameters and filter its unobserved states. When estimating the model, though, LW encountered what is known as a *pile-up problem*, whereby the maximum likelihood estimates of the variances of the innovations to the nonstationary processes z_t and g_t are 0. This is a well-known problem in models with unobserved components that reflects the fact that the sampling distribution of the variance estimates has point mass at zero when T is not too large even though their true values are positive (see Stock, 1994, and Laubach, 2001).

To avoid this problem, HLW17 and HLW23 employ the following sequential estimation method. First, they extract a measure of potential output by estimating a simpler model which assumes that the trend growth rate g_t is constant and omits the real rate gap $r_{t-1} - r^*_{t-1}$ from equation (1). In this respect, they compute the real interest rate as the nominal interest rate net of a four-quarter moving average of past inflation. They also compute Stock and Watson's (1998) median unbiased estimator of $\lambda_g = \sigma_g/\sigma_{y^*}$ by testing for a structural break with unknown break date in equation (6). In a second step, they fix the estimated value of λ_g from the first step, and reintroduced the real interest rate gap in the output gap equation (1) under the assumption that z_t is constant. Again, they obtain Stock and Watson's (1998) median unbiased estimator of $\lambda_z = \gamma\sigma_z/\sigma_{\tilde{y}}$ by testing for a structural break with unknown break date on the IS curve in equation (1). Strictly speaking, reparametrizing σ_z as a function of $\sigma_{\tilde{y}}$, λ_z and γ creates a problem when $\gamma = 0$, but this can always be avoided by reverting to the original reparametrization or by fixing γ to a very small constant. Their third and final step consists of imposing the estimated values of λ_g and λ_z from the first and second steps, respectively, and estimating the remaining model parameters by Gaussian maximum likelihood. Next, we explain how we have modified those three steps to deal with our proposed augmented model:

B.1 Stage 1

First, by omitting the interest rate gap from equation (1) and assuming that the trend growth rate is constant, we estimate a simpler model that recovers a measure of potential

output. Specifically, the state-space representation of this simpler model is

$$\begin{pmatrix} y_t - \bar{g} \\ \pi_t \\ r_t - \bar{g} \end{pmatrix} = \begin{pmatrix} 1 & -\alpha_{y,1} & -\alpha_{y,2} & 0 \\ 0 & -\kappa & 0 & 0 \\ 0 & 0 & 0 & 1 \end{pmatrix} \begin{pmatrix} y_t^* \\ y_{t-1}^* \\ y_{t-2}^* \\ \tilde{r}_t \end{pmatrix}$$

$$+ \begin{pmatrix} \alpha_{y,1} & \alpha_{y,2} & 0 & 0 & \phi & -\phi\alpha_{y,1} & -\phi\alpha_{y,2} \\ \kappa & 0 & \alpha_\pi & 1-\alpha_\pi & 0 & -\phi\kappa & 0 \\ 0 & 0 & 0 & 0 & 0 & 0 & 0 \end{pmatrix} \begin{pmatrix} y_{t-1} - \bar{g} \\ y_{t-2} - \bar{g} \\ \pi_{t-1} \\ \pi_{t-2,4} \\ d_t \\ d_{t-1} \\ d_{t-2} \end{pmatrix} + \begin{pmatrix} \varepsilon_t^y \\ \varepsilon_t^\pi \\ 0 \end{pmatrix},$$

$$\begin{pmatrix} y_t^* \\ y_{t-1}^* \\ y_{t-2}^* \\ \tilde{r}_t \end{pmatrix} = \begin{pmatrix} 1 & 0 & 0 & 0 \\ 1 & 0 & 0 & 0 \\ 0 & 1 & 0 & 0 \\ 0 & 0 & 0 & \alpha_r \end{pmatrix} \begin{pmatrix} y_{t-1}^* \\ y_{t-2}^* \\ y_{t-3}^* \\ \tilde{r}_{t-1} \end{pmatrix} + \begin{pmatrix} \varepsilon_t^{y^*} \\ 0 \\ 0 \\ \varepsilon_t^{\tilde{r}} \end{pmatrix},$$

$$\mathbf{R}_t = \kappa_t^2 \begin{pmatrix} \sigma_{\bar{y}}^2 & 0 & 0 \\ 0 & \sigma_\pi^2 & 0 \\ 0 & 0 & 0 \end{pmatrix} \text{ and } \mathbf{Q} = \begin{pmatrix} \sigma_{y^*}^2 & 0 & 0 & 0 \\ 0 & 0 & 0 & 0 \\ 0 & 0 & 0 & 0 \\ 0 & 0 & 0 & \sigma_{\tilde{r}}^2 \end{pmatrix}.$$

Like HLW17 and HLW23, we initialize the filter using values of potential output obtained by applying the HP filter to log real GDP with smoothing parameter $\lambda = 36{,}000$. Given that in contrast to HLW17 and HLW23, the real interest rate gap $\tilde{r}$ is a state variable in our augmented model, we initialize it at 0. Finally, we initialize the covariance matrix of the state variables as explained in footnote 6 of HLW17.

To help convergence of the estimation algorithm, we impose the following parameter constraints: (i) the slope γ of the IS curve is negative (smaller than -0.0025); (ii) the slope κ of the Phillips curve is positive (larger than 0.025); (iii) the COVID-19 variance-scaling parameters $\kappa_{2020}, \kappa_{2021}$ and κ_{2022} are greater or equal to 1; and (iv) the autoregressive parameter of the interest rate gap must be non explosive $|\alpha_r| \leq 1$. Constraints (i) to (iii) come from HLW23. In addition, when we estimate the confidence bands, we also follow HLW23 in imposing that the parameter draws of $\alpha_{y,1}$ and $\alpha_{y,2}$ add up to less than 1. Each draw is required to satisfy this restriction, as well as the constraints (i) to (iv) above.

Equations (5) and (6) imply a local level model for the first difference of potential output,

$$\begin{aligned} \Delta y_t^* &= g_{t-1} + \varepsilon_t^{y^*}, \\ g_t &= g_{t-1} + \varepsilon_t^g. \end{aligned}$$

Consequently, given an estimate for potential output, we can use Stock and Watson's (1998)

median unbiased estimator of $\lambda_g = \sigma_g/\sigma_{y^*}$, which is obtained by computing the exponential Wald statistic of Andrews and Ploberger (1994), as in HLW17.

B.2 Stage 2

The second step consists of imposing the estimated value of λ_g from the first step, followed by the reintroduction of the real interest rate gap in the output gap equation under the assumption that z_t is a constant equal to $\bar{z}$. The state-space representation of the model becomes

$$\begin{pmatrix} y_t \\ \pi_t \\ r_t \end{pmatrix} = \begin{pmatrix} 1 & -\alpha_{y,1} & -\alpha_{y,2} & 0 & -2c\gamma & -2c\gamma & 0 \\ 0 & -\kappa & 0 & 0 & 0 & 0 & 0 \\ 0 & 0 & 0 & 4c & 0 & 0 & 1 \end{pmatrix} \begin{pmatrix} y_t^* \\ y_{t-1}^* \\ y_{t-2}^* \\ g_t \\ g_{t-1} \\ g_{t-2} \\ \tilde{r}_t \end{pmatrix}$$

$$+ \begin{pmatrix} \alpha_{y,1} & \alpha_{y,2} & \gamma/2 & \gamma/2 & 0 & 0 & \alpha_0 & \phi & -\phi\alpha_{y,1} & -\phi\alpha_{y,2} \\ \kappa & 0 & 0 & 0 & \alpha_\pi & 1-\alpha_\pi & 0 & 0 & -\phi\kappa & 0 \\ 0 & 0 & 0 & 0 & 0 & 0 & 0 & 0 & 0 & 0 \end{pmatrix} \begin{pmatrix} y_{t-1} \\ y_{t-2} \\ r_{t-1} \\ r_{t-2} \\ \pi_{t-1} \\ \pi_{t-2,4} \\ 1 \\ d_t \\ d_{t-1} \\ d_{t-2} \end{pmatrix} + \begin{pmatrix} \varepsilon_t^y \\ \varepsilon_t^\pi \\ 0 \end{pmatrix},$$

$$\begin{pmatrix} y_t^* \\ y_{t-1}^* \\ y_{t-2}^* \\ g_t \\ g_{t-1} \\ g_{t-2} \\ \tilde{r}_t \end{pmatrix} = \begin{pmatrix} 1 & 0 & 0 & 1 & 0 & 0 & 0 \\ 1 & 0 & 0 & 0 & 0 & 0 & 0 \\ 0 & 1 & 0 & 0 & 0 & 0 & 0 \\ 0 & 0 & 0 & 1 & 0 & 0 & 0 \\ 0 & 0 & 0 & 1 & 0 & 0 & 0 \\ 0 & 0 & 0 & 0 & 1 & 0 & 0 \\ 0 & 0 & 0 & 0 & 0 & 0 & \alpha_r \end{pmatrix} \begin{pmatrix} y_{t-1}^* \\ y_{t-2}^* \\ y_{t-3}^* \\ g_{t-1} \\ g_{t-2} \\ g_{t-3} \\ \tilde{r}_{t-1} \end{pmatrix} + \begin{pmatrix} \varepsilon_t^{y^*} \\ 0 \\ 0 \\ \varepsilon_t^g \\ 0 \\ 0 \\ \varepsilon_t^{\tilde{r}} \end{pmatrix},$$

$$\mathbf{R}_t = \kappa_t^2 \begin{pmatrix} \sigma_y^2 & 0 & 0 \\ 0 & \sigma_\pi^2 & 0 \\ 0 & 0 & 0 \end{pmatrix} \text{ and } \mathbf{Q} = \begin{pmatrix} \sigma_{y^*}^2 & 0 & 0 & 0 & 0 & 0 & 0 \\ 0 & 0 & 0 & 0 & 0 & 0 & 0 \\ 0 & 0 & 0 & 0 & 0 & 0 & 0 \\ 0 & 0 & 0 & (\lambda_g \sigma_{y^*})^2 & 0 & 0 & 0 \\ 0 & 0 & 0 & 0 & 0 & 0 & 0 \\ 0 & 0 & 0 & 0 & 0 & 0 & 0 \\ 0 & 0 & 0 & 0 & 0 & 0 & \sigma_{\tilde{r}}^2 \end{pmatrix}.$$

Equations (1), (5), and (8) form a local level model given by

$$\tilde{y}_t - \alpha_{y,1}\tilde{y}_{t-1} - \alpha_{y,2}\tilde{y}_{t-2} + \gamma\frac{r_{t-1}+r_{t-2}}{2} - 4\gamma g_{t-1} = \gamma z_{t-1} + \varepsilon_t^{\tilde{y}},$$
$$z_t = z_{t-1} + \varepsilon_t^z.$$

Once again, we use Stock and Watson's (1998) median unbiased estimator of $\lambda_z = \gamma\sigma_z\sigma_{\tilde{y}}^{-1}$ by testing for a structural break with unknown break date using the exponential Wald statistics of Andrews and Ploberger (1994). When $\gamma = 0$, one can set γ to a small number, or use equation (14) instead of equation (1) to form the alternative local level model:

$$r_t - 4cg_t - \alpha_r\tilde{r}_{t-1} = z_t + \varepsilon_t^{\tilde{r}},$$
$$z_t = z_{t-1} + \varepsilon_t^z,$$

in which case $\lambda_z = \sigma_z/\sigma_{\tilde{r}}$.

As in the first stage, we apply the HP filter to log real GDP with $\lambda = 36{,}000$ and take the values of the trend component thus generated as the initial measure potential output, so that its first difference proxies g. We also initialize the real interest rate gap $\tilde{r}$ to 0 at period 0, and the covariance matrix of the state variables as explained in footnote 6 of HLW17. Finally, we impose the same parameter restrictions as in stage 1.

B.3 Stage 3

The third and final step consists of estimating the full model specified by equations (A3) and (A4) by maximum likelihood but keeping fixed the values of λ_g and λ_z estimated in the first and second steps, respectively.

All the remaining details are as in the previous two stages.

C Log-likelihood comparisons

A key challenge in comparing the log-likelihoods of the original and augmented HLW models is the fact that the baseline model maximizes the likelihood of output and inflation, whereas the augmented model maximizes the likelihood of output, inflation *and* the real interest rate. To compare the fit the two models provide, we focus only on the joint likelihood of output and inflation, which we can obtain by exploiting the properties of the multivariate normal distribution.

Specifically, let $\mathbf{y}_t = (y_t, \pi_t)'$, $\mathbf{y}_t^a = (y_t, \pi_t, r_t)'$, and

$$\mathbf{w}_t = (y_{t-1}, y_{t-2}, r_{t-1}, r_{t-2}, \pi_{t-1}, \pi_{t-2,4}, d_t, d_{t-1}, d_{t-2})'$$

In the baseline model, the prediction equations of the Kalman filter imply that

$$\mathbf{y}_t|\mathbf{w}_t, \mathbf{w}_{t-1}, \ldots \sim N(\mathbf{C}\mathbf{x}_{t|t-1} + \mathbf{D}\mathbf{w}_t, \mathbf{C}\mathbf{P}_{t|t-1}\mathbf{C}' + \mathbf{R}),$$

whence we can easily calculate the sample log-likelihood function by using the prediction error decomposition.

On the other hand, in the augmented model we have that

$$\mathbf{y}_t^a|\mathbf{w}_t, \mathbf{w}_{t-1}, \ldots \sim N(\mathbf{C}^a\mathbf{x}_{t|t-1}^a + \mathbf{D}^a\mathbf{w}_t, \mathbf{C}^a\mathbf{P}_{t|t-1}^a\mathbf{C}^{a\prime} + \mathbf{R}^a).$$

Define the marginalization matrix

$$\mathbf{M} = \begin{pmatrix} 1 & 0 & 0 \\ 0 & 1 & 0 \end{pmatrix}.$$

The joint normality of $\mathbf{y}_t^a|\mathbf{w}_t, \mathbf{w}_{t-1}, \ldots$ implies that the distribution of $\mathbf{y}_t|\mathbf{w}_t, \mathbf{w}_{t-1}, \ldots$ is also (conditionally) normal. Specifically,

$$\mathbf{y}_t|\mathbf{w}_t, \mathbf{w}_{t-1}, \ldots \sim N(\mathbf{M}\mathbf{C}^a\mathbf{x}_{t|t-1}^a + \mathbf{M}\mathbf{D}^a\mathbf{w}_t, \mathbf{M}\mathbf{C}^a\mathbf{P}_{t|t-1}^a\mathbf{C}^{a\prime}\mathbf{M}' + \mathbf{M}\mathbf{R}^a\mathbf{M}').$$

In practice, the matrix $\mathbf{M}$ simply selects the relevant rows and columns of the conditional mean vector and covariance matrix of the distribution of $\mathbf{y}_t^a|\mathbf{w}_t, \mathbf{w}_{t-1}, \ldots$

D Confidence bands for the state vector

Our approach closely follows Hamilton (1986). Consider the estimation of an unobserved state vector $\mathbf{x}_t$ when the true value of the parameter vector $\boldsymbol{\theta}$ is unknown, given the observed data available up to time T, $\mathbf{z}_T$ say, which includes both the endogeneous variables $\mathbf{y}_T$ and the predetermined ones $\mathbf{w}_T$. We take a Bayesian perspective and consider that the parameter vector is a random variable with distribution $\boldsymbol{\theta} \sim N(\boldsymbol{\theta}_0, \boldsymbol{\Sigma}_0)$. We seek to evaluate the variance of the unobserved state vector

$$E\left\{[\mathbf{x}_t - \hat{\mathbf{x}}_t(\mathbf{z}_T)]\,[\mathbf{x}_t - \hat{\mathbf{x}}_t(\mathbf{z}_T)]'\,|\mathbf{z}_T\right\}$$

which can be additively decomposed as

$$\begin{aligned} E\left\{[\mathbf{x}_t - \hat{\mathbf{x}}_t(\mathbf{z}_T)]\,[\mathbf{x}_t - \hat{\mathbf{x}}_t(\mathbf{z}_T)]'\,|\mathbf{z}_T\right\} &= E_{\boldsymbol{\theta}|\mathbf{z}_T}\left\{[\mathbf{x}_t - \hat{\mathbf{x}}_t(\mathbf{z}_T, \boldsymbol{\theta})]\,[\mathbf{x}_t - \hat{\mathbf{x}}_t(\mathbf{z}_T, \boldsymbol{\theta})]'\,|\mathbf{z}_T\right\} + \\ &+ E_{\boldsymbol{\theta}|\mathbf{z}_T}\left\{[\hat{\mathbf{x}}_t(\mathbf{z}_T, \boldsymbol{\theta}) - \hat{\mathbf{x}}_t(\mathbf{z}_T)]\,[\hat{\mathbf{x}}_t(\mathbf{z}_T, \boldsymbol{\theta}) - \hat{\mathbf{x}}_t(\mathbf{z}_T)]'\,|\mathbf{z}_T\right\} \end{aligned}$$

The first term in the right-hand side represents filter uncertainty, while the second term represents parameter uncertainty. To compute the filter uncertainty, generate B draws of the parameter vector from a $N[\hat{\boldsymbol{\theta}}(\mathbf{z}_T), \hat{\boldsymbol{\Sigma}}(\mathbf{z}_T)]$ distribution, where $\hat{\boldsymbol{\theta}}(\mathbf{z}_T)$ is the MLE of $\boldsymbol{\theta}$ and $\hat{\boldsymbol{\Sigma}}(\mathbf{z}_T)$

is its associated asymptotic variance-covariance matrix. For each such draw, $\boldsymbol{\theta}_i$, we calculate the sequences $\{\hat{\mathbf{x}}_t(\mathbf{z}_T, \boldsymbol{\theta}_i)\}$ and $\left\{\hat{\mathbf{P}}_t(\mathbf{z}_T, \boldsymbol{\theta}_i)\right\}$ by means of either the filter or smoother equations of the Kalman filter. Next, we average the $\hat{\mathbf{P}}_t(\mathbf{z}_T, \boldsymbol{\theta}_i)$ across draws for each t, namely

$$\frac{1}{B}\sum_{i=1}^{B}\hat{\mathbf{P}}_t(\mathbf{z}_T, \boldsymbol{\theta}_i), \tag{D5}$$

which yields a Monte Carlo estimate of the contribution of the filter uncertainty. Then, we calculate the variance of $\hat{\mathbf{x}}_t(\mathbf{z}_T, \boldsymbol{\theta}_i)$ across draws for the same t as

$$\frac{1}{B}\sum_{i=1}^{B}\left[\hat{\mathbf{x}}_t(\mathbf{z}_T, \boldsymbol{\theta}_i) - \hat{\mathbf{x}}_t(\mathbf{z}_t)\right]\left[\hat{\mathbf{x}}_t(\mathbf{z}_T, \boldsymbol{\theta}_i) - \hat{\mathbf{x}}_t(\mathbf{z}_t)\right]', \tag{D6}$$

which yields an estimate of the parameter uncertainty. Finally, we compute the estimated total variance by adding up (D5) and (D6).

D.1 Differences with HLW23

These are the main differences with the manner in which HLW23 compute their confidence bands for the state variables:

1. We provide confidence bands for the filtered values of z_t, which are more appropriate for real time analysis, rather than the smoothed estimates.

2. We take into account the fact that the parameter c is freely estimated when computing the filter uncertainty of r_t^*. Specifically, let $\hat{\mathbf{P}}_t^B$ be the MSE of the forecast of the state variables averaged across the random draws:

   $$\hat{\mathbf{P}}_t^B = \frac{1}{B}\sum_{i=1}^{B}\hat{\mathbf{P}}_t(\mathbf{z}_T, \boldsymbol{\theta}_i)$$

   Given that in the R code posted on the NY Fed webpage $r_t^* = 4cg_t + z_t$ even though HLW23 exclude the 4 in the paper, we compute the contribution of filter uncertainty as:

   $$\frac{1}{B}\sum_{i=1}^{B}16c_i^2\hat{\mathbf{P}}_t(\mathbf{z}_T, \boldsymbol{\theta}_i)[g,g] + \hat{\mathbf{P}}_t(\mathbf{z}_T, \boldsymbol{\theta}_i)[z,z] + 8c_i\hat{\mathbf{P}}_t(\mathbf{z}_T, \boldsymbol{\theta}_i)[g,z]$$

   where c_i denotes the i^{th} draw of the parameter c and $\hat{\mathbf{P}}_t(\mathbf{z}_T, \boldsymbol{\theta}_i)[g,g]$, $\hat{\mathbf{P}}_t(\mathbf{z}_T, \boldsymbol{\theta}_i)[z,z]$ and $\hat{\mathbf{P}}_t(\mathbf{z}_T, \boldsymbol{\theta}_i)[g,z]$ the relevant elements of the estimated matrix of MSEs.

   In contrast, they use:

   $$\frac{1}{B}\sum_{i=1}^{B}16\hat{\mathbf{P}}_t(\mathbf{z}_T, \boldsymbol{\theta}_i)[g,g] + \hat{\mathbf{P}}_t(\mathbf{z}_T, \boldsymbol{\theta}_i)[z,z],$$

   which implicitly assumes $c_i = 1$ for all i.

E Observability

E.1 Definition

Consider the general state space form in Harvey (1989) for $\mathbf{y}_t$, an n-variate time series observed at date t,

$$\mathbf{y}_t = \mathbf{C}\mathbf{x}_t + \mathbf{D}\mathbf{w}_t + \mathbf{u}_t, \qquad \mathbf{u}_t \sim N(\mathbf{0}, \mathbf{R}), \tag{E7}$$

$$\mathbf{x}_t = \mathbf{A}\mathbf{x}_{t-1} + \mathbf{v}_t, \qquad \mathbf{v}_t \sim N(\mathbf{0}, \mathbf{Q}), \tag{E8}$$

where $\mathbf{x}_t$ is an $s \times 1$ vector of unobserved states, $\mathbf{w}_t$ a $p \times 1$ vector of (observed) exogenous or predetermined variables; $\mathbf{C}$, $\mathbf{D}$, and $\mathbf{A}$ matrices of parameters of dimension $n \times s$, $n \times p$, and $s \times s$, respectively; $\mathbf{u}_t$ an $n \times 1$ vector of zero-mean serially uncorrelated measurement errors with covariance matrix $\mathbf{R}$; and finally $\mathbf{v}_t$ an $s \times 1$ vector of zero-mean serially uncorrelated disturbances with covariance matrix $\mathbf{Q}$, uncorrelated to $\mathbf{u}_t$ at all leads and lags. This representation is slightly different from the one in (9) and (10) in the timing of the state variables in the measurement equation, but it is more appropriate for the discussion of the observability of the HLW and augmented models, whose measurement equations are (A1) and (A3), respectively.

In section 3, we stated that the linear system (E7)-(E8) will be observable if and only if the following condition holds

$$\operatorname{rank} \begin{bmatrix} \mathbf{C} \\ \mathbf{CA} \\ \mathbf{CA}^2 \\ \vdots \\ \mathbf{CA}^{s-1} \end{bmatrix} = s. \tag{E9}$$

In what follows, we will provide an intuitive justification for this necessary and sufficient condition. A crucial insight behind the idea of observability in Kalman (1960) is that the problem of determining the path of the state vector $\mathbf{x}_t$ for $t \geq 1$ can be simplified to the problem of finding the initial condition $\mathbf{x}_0$. Once we know this condition, we can recover the subsequent path of the state variables by exploiting the recursions of the transition equation in (E8) and our knowledge of the disturbances $\mathbf{v}_t$.

Given that the s-dimensional vector $\mathbf{x}_0$ contains s unknown components, one would expect that s observations are sufficient to determine $\mathbf{x}_0$. Take $t = 0, 1, \ldots, s-1$ and generate the following sequence:

$$
\begin{aligned}
\mathbf{y}_0 &= \mathbf{C}\mathbf{x}_0 + \mathbf{D}\mathbf{w}_0 + \mathbf{u}_0, \\
\mathbf{y}_1 &= \mathbf{C}\mathbf{x}_1 + \mathbf{D}\mathbf{w}_1 + \mathbf{u}_1 = \mathbf{C}\mathbf{A}\mathbf{x}_0 + \mathbf{C}\mathbf{v}_1 + \mathbf{D}\mathbf{w}_1 + \mathbf{u}_1, \\
\mathbf{y}_2 &= \mathbf{C}\mathbf{x}_2 + \mathbf{D}\mathbf{w}_2 + \mathbf{u}_2 = \mathbf{C}\mathbf{A}^2\mathbf{x}_0 + \mathbf{C}\mathbf{A}\mathbf{v}_1 + \mathbf{C}\mathbf{v}_2 + \mathbf{D}\mathbf{w}_2 + \mathbf{u}_2, \\
&\vdots \\
\mathbf{y}_{s-1} &= \mathbf{C}\mathbf{x}_{s-1} + \mathbf{D}\mathbf{w}_{s-1} + \mathbf{u}_{s-1} = \mathbf{C}\mathbf{A}^{s-1}\mathbf{x}_0 + \sum_{j=1}^{s-1} \mathbf{C}\mathbf{A}^{s-1-j}\mathbf{v}_j + \mathbf{D}\mathbf{w}_{s-1} + \mathbf{u}_{s-1},
\end{aligned}
$$

which can be compactly written as

$$
\begin{bmatrix} \mathbf{C} \\ \mathbf{C}\mathbf{A} \\ \mathbf{C}\mathbf{A}^2 \\ \vdots \\ \mathbf{C}\mathbf{A}^{s-1} \end{bmatrix} \mathbf{x}_0 = \begin{bmatrix} \mathbf{y}_0 \\ \mathbf{y}_1 \\ \mathbf{y}_2 \\ \vdots \\ \mathbf{y}_{s-1} \end{bmatrix} + \boldsymbol{\Gamma} \begin{bmatrix} \mathbf{v}_0 \\ \mathbf{v}_1 \\ \mathbf{v}_2 \\ \vdots \\ \mathbf{v}_{s-1} \end{bmatrix} + \boldsymbol{\Delta} \begin{bmatrix} \mathbf{w}_0 \\ \mathbf{w}_1 \\ \mathbf{w}_2 \\ \vdots \\ \mathbf{w}_{s-1} \end{bmatrix} + \begin{bmatrix} \mathbf{u}_0 \\ \mathbf{u}_1 \\ \mathbf{u}_2 \\ \vdots \\ \mathbf{u}_{s-1} \end{bmatrix} \tag{E10}
$$

where $\boldsymbol{\Gamma}$ and $\boldsymbol{\Delta}$ are $s \times s^2$ and $s \times ps$ matrices, respectively, which depend on $\mathbf{C}$, $\mathbf{A}$ and $\mathbf{D}$. Interestingly, the rows of the matrix that multiplies $\mathbf{x}_0$ contain the impulse-response coefficients that measure the impact of the shocks to the state variables $\mathbf{v}_t$ on the observed ones $\mathbf{y}_{t+j}$ for $j = 0, \ldots, s-1$. Given perfect knowledge of the realizations of the observables and disturbances that enter in the right-hand-side of (E10), the system contains s linear equations in the s unknowns in $\mathbf{x}_0$. Therefore, the solution to this system will be unique if and only if the matrix which premultiplies $\mathbf{x}_0$, known as the *observability matrix*, has rank equal to the number of unknowns, s. If we denote such a matrix by $\mathbf{O}$, then the system (E10) can be written as

$$
\mathbf{O}\mathbf{x}_0 = \boldsymbol{\Psi}
$$

If $\text{rank}(\mathbf{O}) = s$, then the matrix $\mathbf{O}'\mathbf{O}$ is invertible, and the unique solution to the system will be

$$
\mathbf{x}_0 = \left(\mathbf{O}'\mathbf{O}\right)^{-1} \mathbf{O}'\boldsymbol{\Psi}.
$$

Thus, we can recover the unique path for the state vector, $\mathbf{x}_t$ given the transition equation in (E8) and perfect knowledge of the disturbances $\mathbf{v}_t$. In contrast, if $\text{rank}(\mathbf{O}) < s$, then the matrix $\mathbf{O}'\mathbf{O}$ is not invertible, and there are infinite solutions for $\mathbf{x}_0$ that satisfy (E10). As a result, we cannot recover a unique path for the state vector, and the model is said to be unobservable.

Finally, it is worth mentioning that the observability matrix is constructed using powers of $\mathbf{A}$ only up to $\mathbf{A}^{s-1}$. This is justified by the Cayley-Hamilton theorem, which implies that $\mathbf{A}^{s+j}$ for $j \geq 0$ will be a linear combination of $\mathbf{A}^0$ through $\mathbf{A}^{s-1}$. Consequently, augmenting $\mathbf{O}$ in (11) with further powers of $\mathbf{A}$ cannot increase its rank.

E.2 Additional examples

For pedagogical reasons, next we consider the observability properties of some simple state space models that are popular in macroeconomics.

E.2.1 Local Level Model

Consider a local level model as in Watson (1986), according to which a univariate observed process, y_t, is the sum of a permanent component, y_t^*, and a transitory component $\tilde{y}_t$,

$$\begin{aligned} y_t &= y_t^* + \tilde{y}_t, \\ y_t^* &= y_{t-1}^* + \varepsilon_t^{y^*}, \qquad \varepsilon_t^{y^*} \sim N(0, \sigma_{y^*}^2), \\ \tilde{y}_t &= \alpha \tilde{y}_{t-1} + \varepsilon_t^{\tilde{y}}, \qquad \varepsilon_t^{\tilde{y}} \sim N(0, \sigma_{\tilde{y}}^2), \end{aligned}$$

where we allow for a serially correlated transitory component with correlation coefficient that satisfies $|\alpha| < 1$. We can think of y_t as of the output level, with y_t^* being its potential level, and $\tilde{y}_t$ the output gap. We can then cast the model is state space form as

$$\begin{aligned} y_t &= \underbrace{\begin{bmatrix} 1 & 1 \end{bmatrix}}_{\mathbf{C}} \begin{bmatrix} y_t^* \\ \tilde{y}_t \end{bmatrix}, \\ \begin{bmatrix} y_t^* \\ \tilde{y}_t \end{bmatrix} &= \underbrace{\begin{bmatrix} 1 & 0 \\ 0 & \alpha \end{bmatrix}}_{\mathbf{A}} \begin{bmatrix} y_{t-1}^* \\ \tilde{y}_{t-1} \end{bmatrix} + \begin{bmatrix} \varepsilon_t^{y^*} \\ \varepsilon_t^{\tilde{y}} \end{bmatrix}. \end{aligned}$$

Thus, the observability matrix of this system with two state variables is

$$\mathbf{O} = \begin{bmatrix} \mathbf{C} \\ \mathbf{CA} \end{bmatrix} = \begin{bmatrix} 1 & 1 \\ 1 & \alpha \end{bmatrix}.$$

The model is observable if the observability matrix has full rank, which always happens given that $|\alpha| < 1$. In contrast, if $\alpha = 1$, then the observability matrix is rank deficient and the model is not observable. Intuitively, the observed process y_t is the sum of two nonstationary processes that cannot be separately told apart.

Notice that we could have also written the model according to the following alternative state space representation,

$$\begin{aligned} y_t &= (1-\alpha) y_{t-1}^* + \alpha y_{t-1} + \varepsilon_t^{\tilde{y}} + \varepsilon_t^{y^*}, \\ y_t^* &= y_{t-1}^* + \varepsilon_t^{y^*}, \end{aligned}$$

where the state vector includes y_{t-1}^*only. In this case, the observability matrix boils down to a scalar equal to $1 - \alpha$. As before, the model is observable as long as $|\alpha| < 1$. This confirms that

the specific choice of the state space representation does not affect the observability properties of the original model.

E.2.2 Local Linear Trend Model

Now consider a local linear trend model,

$$\begin{aligned} y_t &= y_t^* + \tilde{y}_t, \\ y_t^* &= y_{t-1}^* + g_{t-1} + \varepsilon_t^{y^*}, \qquad \varepsilon_t^{y^*} \sim N(0, \sigma_{y^*}^2), \\ g_t &= g_{t-1} + \varepsilon_t^g, \qquad \varepsilon_t^g \sim N(0, \sigma_g^2), \\ \tilde{y}_t &= \alpha \tilde{y}_{t-1} + \varepsilon_t^{\tilde{y}}, \qquad \varepsilon_t^{\tilde{y}} \sim N(0, \sigma_{\tilde{y}}^2), \end{aligned}$$

where we restrict the transitory component to be stationary by imposing $|\alpha| < 1$. This model implies that the process for y_t is integrated of order two because potential output depends on trend growth, g_t, which in turn follows a random walk. We can write the model in state-space form as

$$\begin{aligned} y_t &= \underbrace{\begin{bmatrix} 1 & 0 & 1 \end{bmatrix}}_{\mathbf{C}} \begin{bmatrix} y_t^* \\ g_t \\ \tilde{y}_t \end{bmatrix}, \\ \begin{bmatrix} y_t^* \\ g_t \\ \tilde{y}_t \end{bmatrix} &= \underbrace{\begin{bmatrix} 1 & 1 & 0 \\ 0 & 1 & 0 \\ 0 & 0 & \alpha \end{bmatrix}}_{\mathbf{A}} \begin{bmatrix} y_{t-1}^* \\ g_{t-1} \\ \tilde{y}_{t-1} \end{bmatrix} + \begin{bmatrix} \varepsilon_t^{y^*} \\ \varepsilon_t^g \\ \varepsilon_t^{\tilde{y}} \end{bmatrix}. \end{aligned}$$

Thus, the observability matrix of this system with three state variables is

$$\mathbf{O} = \begin{bmatrix} \mathbf{C} \\ \mathbf{CA} \\ \mathbf{CA}^2 \end{bmatrix} = \begin{bmatrix} 1 & 0 & 1 \\ 1 & 1 & \alpha \\ 1 & 2 & \alpha^2 \end{bmatrix}.$$

As before, the model meets the observability condition $\text{rank}(\mathbf{O}) = 3$ if and only if $|\alpha| < 1$. Again, in the special case that $\alpha = 1$, it is easy to see that the first and third columns of the $\mathbf{O}$ matrix, which are associated to the y_t^* and $\tilde{y}_t$ processes, will be equal. Therefore, the observability matrix will be rank deficient and the model is not observable because it is not possible to separately identify potential output from the output gap.

E.2.3 Local Linear Trend Model with a Supply Equation

Consider the following local linear trend model for output augmented with a supply equation that relates inflation, π_t, to past realizations of the output gap as follows:

$$
\begin{aligned}
y_t &= y_t^* + \tilde{y}_t, \\
y_t^* &= y_{t-1}^* + g_{t-1} + \varepsilon_t^{y^*}, \qquad \varepsilon_t^{y^*} \sim N(0, \sigma_{y^*}^2), \\
g_t &= g_{t-1} + \varepsilon_t^g, \qquad \varepsilon_t^g \sim N(0, \sigma_g^2), \\
\tilde{y}_t &= \alpha \tilde{y}_{t-1} + \varepsilon_t^{\tilde{y}}, \qquad \varepsilon_t^{\tilde{y}} \sim N(0, \sigma_{\tilde{y}}^2), \\
\pi_t &= \kappa \tilde{y}_{t-1} + \varepsilon_t^{\pi}, \qquad \varepsilon_t^{\pi} \sim N(0, \sigma_{\pi}^2),
\end{aligned}
$$

where we assume once again that $|\alpha| < 1$. This model is similar to the HLW model, with the only difference that in the latter the output gap also depends on the interest rate gap. It is also similar in spirit to Kuttner (1994), which employs a local level model for output augmented by a supply equation. We can write the model in state space form as

$$
\begin{bmatrix} y_t \\ \pi_t \end{bmatrix} = \underbrace{\begin{bmatrix} 1 & 0 & \alpha \\ 0 & 0 & -\kappa \end{bmatrix}}_{\mathbf{C}} \begin{bmatrix} y_t^* \\ g_t \\ \tilde{y}_{t-1} \end{bmatrix} + \begin{bmatrix} \varepsilon_t^{\tilde{y}} \\ \varepsilon_t^{\pi} \end{bmatrix},
$$

$$
\begin{bmatrix} y_t^* \\ g_t \\ \tilde{y}_{t-1} \end{bmatrix} = \underbrace{\begin{bmatrix} 1 & 1 & 0 \\ 0 & 1 & 0 \\ 0 & 0 & \alpha \end{bmatrix}}_{\mathbf{A}} \begin{bmatrix} y_{t-1}^* \\ g_{t-1} \\ \tilde{y}_{t-2} \end{bmatrix} + \begin{bmatrix} \varepsilon_t^{y^*} \\ \varepsilon_t^{g} \\ \varepsilon_{t-1}^{\tilde{y}} \end{bmatrix}.
$$

Thus, the observability matrix of this system with three state variables is

$$
\mathbf{O} = \begin{bmatrix} \mathbf{C} \\ \mathbf{CA} \\ \mathbf{CA}^2 \end{bmatrix} = \begin{bmatrix} 1 & 0 & \alpha \\ 0 & 0 & -\kappa \\ 1 & 1 & \alpha^2 \\ 0 & 0 & -\alpha\kappa \\ 1 & 2 & \alpha^3 \\ 0 & 0 & -\alpha^2\kappa \end{bmatrix}.
$$

Let us consider two cases. First, suppose that $\kappa = 0$, so that the model boils down to the standard local linear trend model. In this case, the observability matrix has full rank because $|\alpha| < 1$, as previously shown. Second, consider now the special case $\alpha = 1$, so that the output gap, $\tilde{y}_t$, is nonstationary. We can still uniquely determine the state vector as long as $\kappa \neq 0$. Intuitively, inflation provides valuable information for the output gap because past realizations of this variable have an effect on current inflation.

Finally, it is worth emphasizing that the observability conclusions do not change if we cast the model in a different state space representation. In particular, given the identity that defines the output gap, once we know potential output we also know the output gap.